Elucidating the Early Stages of Keratin Filament Assembly

Pierre A. Coulombe and Elaine Fuchs

Howard Hughes Medical Institute, Departments of Molecular Genetics and Cell Biology and of Biochemistry and Molecular Biology, The University of Chicago, Chicago, IL 60637

Abstract. Because of extraordinarily tight coiled-coil associations of type I and type II keratins, the composition and structure of keratin subunits has been difficult to determine. We report here the use of novel genetic and biochemical methods to explore the early stages of keratin filament assembly. Using bacterially expressed human K5 and K14, we show that remarkably, these keratins behave as 1:1 complexes even in 9 M urea and in the presence of a reducing agent. Gel filtration chromatography and chemical cross-linking were used to identify heterodimers and heterotetramers as the most stable building blocks of keratin filament assembly. EM suggested that the dimer consists of a coiled-coil of K5 and K14 aligned in register and in parallel fashion, and the tetramer consists of two dimers in antiparallel fashion, without polarity. In 4 M urea, both end-to-end and lateral packing of tetramers occurred, leading to a variety of larger heteromeric complexes. The coexistence of multiple, higher-ordered associations under strongly denaturing conditions suggests that there may not be a serial sequence of events leading to the assembly of keratin intermediate filaments, but rather a number of associations may take place in parallel.

INTERMEDIATE filaments (IFs)[1] are composed of proteins (molecular mass range 40–210 kD) that self-assemble into complex 8–12-nm cytoskeletal fibers (for reviews, see Steinert et al., 1985; Fuchs et al., 1987; Weber and Geisler, 1987). Based on structure, IF subunits belong to a large class of proteins, including tropomyosin (McLachlan and Stewart, 1975), myosin (Quinlan and Stewart, 1987), and leucine-zipper transcription factors (Landshulz et al., 1988), all of which have α-helical domains that associate to form coiled-coil dimers (Pauling and Corey, 1953; Crick, 1953). The unique feature driving the assembly of coiled-coils is a heptad repeat of hydrophobic residues, where the first and fourth amino acids of every seven in the α-helical sequence are hydrophobic (McLachlan and Stewart, 1975). In the case of transcription factors, the stretches of coiled-coil–forming helices are short, with only 28 residues, or four coiled-coil units (Landshulz et al., 1988). In contrast, IF subunits have long coiled-coil domains: the central α-helical portion of cytoskeletal IF proteins is 310 amino acid residues long (Geisler and Weber, 1982; Hanukoglu and Fuchs, 1982), while the nuclear lamins have a 350 amino acid coiled-coil domain (McKeon et al., 1986; Fisher et al., 1986). At least in part, the long coiled-coil domains of IFs lead to very stable intermolecular associations.

Of proteins forming coiled-coil structures, keratins are the most complex, constituting a group of >20 proteins. A subgroup of IF proteins, keratins can be further divided into two distinct classes based upon their amino acid sequence within the 310 residue α-helical domains: type I and type II α-heli-

cal segments share only ∼25–35% sequence identity, depending upon the particular keratins within each class (Fuchs et al., 1981; Hanukoglu and Fuchs, 1982, 1983; Crewther et al., 1983; Steinert et al., 1983, 1984; Jorcano et al., 1984a,b). In contrast to other IF proteins, which can assemble into homopolymers, keratin filaments have a strict requirement for equimolar amounts of both types of keratins. This is true both in vitro (Franke et al., 1983; Hatzfeld and Franke, 1985) and in vivo (Giudice and Fuchs, 1987). Although type I and type II keratins are expressed as specific pairs in vivo (for review, see Sun et al., 1984), in vitro, almost any type I keratin can be combined with any type II keratin to form 10-nm filaments (Franke et al., 1983; Hatzfeld and Franke, 1985).

It is now widely accepted that the basic structure of IFs is highly similar and that the IF coiled-coil is a dimer. The suggestion of a dimer subunit was originally based on chemical cross-linking studies (Ahmadi and Speakman, 1978; Woods and Inglis, 1984; Quinlan and Franke, 1982; Quinlan et al., 1984, 1986) and model building (Parry et al., 1977; McLachlan, 1978). Recently, dimers of nuclear lamins have been visualized by EM. The polypeptides associate in parallel and in register, to form a ∼50-nm coiled-coil rod. The nonhelical COOH-terminal end domain is larger than the nonhelical NH₂-terminal domain, and can be seen as a globular "head," thereby producing a lollipop-like structure (Aebi et al., 1986; Parry et al., 1987). For desmin, Fab fragment-decorated tetramers appear as 50-nm dumb-bell-like structures, suggesting that dimers interact in an antiparallel fashion and in register (Geisler et al., 1985). In some cases, tetramers with partially staggered, antiparallel

---

1. *Abbreviations used in this paper:* IB, inclusion body; IBF, IB-rich fraction; IF, intermediate filament.

153

dimer configurations have been reported (Ip et al., 1985; Kaufman et al., 1985; Potschka, 1986; Fraser et al., 1987; Stewart et al., 1989), leaving the physiological state of the functional tetramer unresolved. This is an important issue, since in order to account for a 22–25-nm repeat visible in electron micrographs of IFs, the building block of IFs most likely has a half-staggered subunit configuration: if this is not at the dimer or tetramer stage, the stagger is likely to be achieved in either a higher-ordered subunit (e.g., an octamer) or in the packing of tetramers into the IF (for reviews, see Aebi et al., 1988).

Much of what we know about the composition and structure of the IF dimer and tetramer was obtained using the more soluble desmin, vimentin, or lamin proteins. Work with keratin subunits has been greatly hampered by the fact that they form extraordinarily stable complexes with one another (Crewther et al., 1983; Franke et al., 1983; Hatzfeld and Franke, 1985; Eichner et al., 1986). Consequently, it has not only been difficult to purify individual keratins, but it has also been difficult to examine the basic building blocks of keratin filaments. In a paper of major significance, Quinlan et al. (1984) described the isolation of keratin tetramers using 4 M urea and a reducing agent. These complexes contained two each of type I and type II proteins. Under these conditions, type I or type II keratins by themselves also seemed to form intermolecular associations, having sedimentation characteristics of homodimers (Hatzfeld and Franke, 1985; Quinlan et al., 1986; Hatzfeld et al., 1987). While the existence of heterotetramers has been suggested independently on the basis of chemical cross-linking studies (Ahmadi and Speakman, 1978; Woods and Inglis, 1984; Quinlan and Franke, 1982; Quinlan et al., 1984, 1986; Eichner et al., 1986), the significance of the homodimers detected in 4 M urea is still uncertain, since analyses of helical particles from proteolytic digests of wool and murine epidermal keratin IFs have indicated that the keratin coiled-coil might be a heterodimer (Woods and Inglis, 1984; Parry et al., 1985). Moreover, in a recent paper by Hatzfeld and Weber (1990), homodimers appeared to form under certain conditions, but heterodimers of genetically modified K8 and K18 occurred under more stringent conditions, and appeared to be the only form capable of filament formation. Elucidating the basic subunit composition and structure of the keratin dimer and tetramer is a fundamental prerequisite to elucidating the nature of the homo- and hetero-polypeptide interactions involved in keratin IFs. While understanding the basic subunit structures of any IF protein is a prerequisite to elucidating the complex interactions underlying the self-assembly of intermediate filaments, understanding the basis of type I and type II keratin associations is particularly important for two additional reasons (a) the state of the dimer determines whether or not the keratin heterotetramer will have polarity: heterodimers would give rise to nonpolar heterotetramers, whereas homodimers would generate polar heterotetramers; and (b) type I/type II keratin subunits are among the most stable of all inter-chain interactions thus far known in nature, and whether the coiled-coil is a homodimer or heterodimer is a prerequisite to understanding the basis for the extraordinary intermolecular associations involved, and the unique interdependency of type I and type II keratins.

To probe the composition and structure of the building

blocks of keratin filaments, we focused on K5 (58 kD) and K14 (50 kD), type II and type I keratins, respectively, that are expressed in the basal layer of most stratified squamous epithelia (Nelson and Sun, 1983). To circumvent difficulties imposed by strong intermolecular interactions between type I and type II keratins, we over-expressed full-length human K5 and K14 keratins separately in bacteria, which have no endogenous IF networks. Using anion exchange and gel filtration chromatography in the presence of denaturing or partially denaturing conditions, we have been able to isolate and examine populations of keratin monomers, dimers, and tetramers, and to begin to probe the hierarchy of their higher ordered interactions. Using PAGE, chemical cross-linking, and EM, we have determined the composition and structure of these subunits, and have examined the early stages of higher ordered packing of these subunits. Finally, we have reconstituted IFs from these populations, indicating that the subunits we have isolated are bona fide building blocks of keratin IFs. Collectively, our data reveal interesting and novel insights into the composition, structure, and assembly of the basic coiled-coil subunits of keratin filaments. While the denaturing conditions which we used in our approach were much more stringent than those required for most coiled-coil structures, the basic concepts of our approach should be widely, if not universally, applicable to the study of other coiled-coil proteins.

Materials and Methods

Plasmids

pET-K14. An intronless, near full-length human K14 cDNA was constructed as a hybrid from a cloned cDNA (Hanukoglu and Fuchs, 1982) and the corresponding gene (Marchuk et al., 1984). This cDNA was contained within a 2.0-kb Pst I-Sac I fragment, and extended from 9 nucleotides 3' of the ATG translation start codon of human K14 cDNA to ~450 nucleotides 3' of the polyadenylation signal of the human K14 gene. The fragment was first subcloned into the Pst I-SacI sites of the multiple cloning region of plasmid pGEM5zf (Promega Biotec, Madison, WI). This plasmid has an Nco I site (CCATGG) conveniently located just 5' to the Pst I site. To place the ATG sequence of the Nco I site in-frame with the K14 coding sequence, the hybrid vector was linearized with Nco I, followed by DNA polymerase to fill in the ends, followed by Not I digestion, followed by Mung Bean exonuclease digestion of the 3' extended ends, followed by ligation of the plasmid with T4 DNA ligase. The K14 fragment containing the ATG translation initiation codon was then excised from this hybrid plasmid with Nco I and Mlu I endonuclease digestion. The fragment was inserted into the Nco I-Bam HI sites of plasmid pET-8c (Studier and Moffat, 1986), and the plasmid, pETK14 (6.5 kb) was transformed into E. coli strains HMS174 (control) and BL21(DE3)pLysS (containing the T7 RNA polymerase gene). The nucleotide sequence flanking the ATG site of the resulting plasmid was confirmed by sequencing. As a result of the cloning strategy, the first two amino acids of the human K14 cDNA, Thr-Thr, were changed to a single Ala residue.

pET-K5. An intronless, full-length cDNA for human K5 in Bluescript KS+ (Stratagene Cloning Systems, La Jolla, CA) was constructed as a hybrid between a near full-length cDNA (Lersch and Fuchs, 1988) and the corresponding gene (Lersch et al., 1989). An Nco I site was engineered at the beginning of the coding segment by using oligonucleotide-directed mutagenesis. This changed the sequence at the beginning of the coding segment from CCATGT to CCATGG, resulting in a change in the codon of the first amino acid residue of K5 from Ser to Ala. The change was confirmed by DNA sequence analysis, and it enabled the use of partial enzyme digestion to excise the full-length cDNA as a single 1.83-kb Nco I fragment. This fragment was inserted into the Nco I site of plasmid pET-8c (Studier and Moffatt, 1986), to generate pET-K5 (6.3 kb). The plasmid was subsequently used to transform E. coli strains HMS174 and BL21(DE3)pLysS (Studier and Moffatt, 1986).

Overexpression of Keratins in E. coli

Plasmid pET-8c is a derivative of pET-7 (Rosenberg et al., 1987), and it has a T7 RNA polymerase promoter located just 5' from an Nco I site (Studier and Moffatt, 1986). Bacterial strain BL21 (DE3) pLys S contains a cloned chromosomal copy of T7 RNA polymerase under the control of the lacUV5 promoter (Studier and Moffatt, 1986). When induced with IPTG, the T7 polymerase gene is expressed, leading to induction of the target gene/cDNA inserted into pET-8c.

Bacterial clones of BL21(DE3)pLys, transformed with plasmids pET-K5 or pET-K14 were cultured in the presence of M9LB medium supplemented with 0.2% (wt/vol) glucose, 10 mM MgSO$_4$, and 1 mM CaCl$_2$ (Studier and Moffatt, 1986). At an A$_{600}$ of 1, corresponding to ~5 × 10^8–1 × 10^9 cells/ml, induction of keratin expression was achieved by adding isopropyl-β-D-thiogalactopyranoside to the medium to a final concentration of 2.0 mM. After 16–20 h with further shaking, bacteria were harvested by centrifugation. Typically, 10 g of bacteria were obtained per liter of culture.

The specificity of keratin expression was evaluated by PAGE and immunoblot analyses of total protein extracts of the BL21(DE3) cells transformed with either pET-K5 or pET-K14. Antisera used were either anti-K5 (a rabbit polyclonal antiserum against a synthetic peptide corresponding to the 7 COOH-terminal amino acid residues of human K5; Lersch and Fuchs, unpublished observations) or anti-K14 (a rabbit polyclonal antiserum against a COOH-terminal peptide of human K14; Stoler et al., 1988). For controls, we used protein extracts from (a) pET-keratin transformants of HMS174, an E. coli strain that does not contain the cloned T7 RNA polymerase gene; and (b) BL21(DE3)pLysS bacteria transformed with either pET-8c, pET-K5-o.f., in which the K5 coding sequence was out-of-frame with respect to the ATG translation start codon, or pET-K14-o.f., in which the K14 coding sequence was out-of-frame with respect to the ATG translation start codon.

FPLC Purification of Keratins from Bacterial Extracts

Purification of keratins from total bacterial proteins was achieved in three steps. First, an inclusion body (IB)-rich fraction (IBF) was prepared from the frozen bacterial cells using the method of Nagai and Thogersen (1987). The final pellet consisting predominantly of keratin-containing IBs was solubilized in a freshly prepared solution of 6 M urea, 50 mM Tris HCl, 2 mM DTT, 0.3 mg/ml phenyl methyl sulfonyl fluoride, pH 8.1 (i.e., the anion exchange running buffer; see below). The concentration of proteins was adjusted to 5–10 mg/ml as required, and the IBFs were stored at −70°C until needed. This procedure resulted in a keratin fraction that was ~35–40% pure.

To further purify keratins, we used an inert (i.e., titanium-coated) HPLC system manufactured by Pharmacia-LKB (Piscataway, NJ). IBF extracts (~5–10 mg protein) were first passaged through a 1-ml Mono-Q anion exchange column (Pharmacia-LKB). The anion exchange running buffer (see above) was pumped at a flow rate of 0.5 ml/min. Keratins were eluted with a 25-ml gradient of 0–200 mM guanidine-HCl (Hatzfeld and Franke, 1985), run at 0.5 ml/min. 500-μl fractions were collected, and analyzed by SDS-PAGE and Coomassie Blue staining. Peak fractions were then pooled and stored at −70°C until needed. Before use, samples were concentrated by ultrafiltration through Centricon-10 units, as specified by the manufacturer (Amicon; W.R. Grace & Co., Boston, MA).

Final purification of keratins was accomplished by subjecting the concentrated fractions obtained above to gel filtration chromatography. For purification of keratin monomers, we used a Superose 12 column (Pharmacia-LKB), and a running buffer of 6 M urea, 50 mM Tris HCl, 10 mM β-mercaptoethanol, 0.3 mg/ml PMSF, pH 7.4. Samples were pumped at 0.1 ml/min, and 100-μl fractions were collected. Fractions were analyzed by SDS-PAGE, and fractions containing pure keratins were pooled and concentrated as described above.

In Vitro Reconstitution of 10-nm Filaments

Essentially, the procedure of Franke et al. (1982) was followed. Keratin complexes were first equilibrated by dialysis against a urea buffer consisting of 50 mM Tris-HCl, 10 mM β-mercaptoethanol, 0.3 mg/ml PMSF, pH 7.25, containing either 6 or 9 M urea, for 2 h at room temperature. Additional dialyses were performed with 10 mM Tris HCl, 10 mM β-mercaptoethanol, pH 7.25, for 2 h at room temperature, followed by 12 h at 4°C, and finally 50 mM Tris HCl, 10 mM β-mercaptoethanol, pH 7.25, for 12 h at 4°C. Preparations were then stored at 4°C until examined under a Philips CM10 electron microscope.

Keratin Complex Formation and Isolation

Pure preparations of K5 and K14 in either 6 or 9 M urea buffers were obtained by FPLC chromatography, as described above. For the 9 M urea samples, the buffer systems used were identical to the 6 M urea ones. K5- or K14-rich fractions were pooled, and the protein concentration measured using an assay kit (Bio-Rad Laboratories, Richmond, CA). K5 and K14 were then mixed in the desired ratio in a final volume of 1.5 ml and at a final concentration of 1.0–1.2 mg/ml. After 30 min at room temperature, K5-K14 mixtures were stored at 4°C until further processed. K5-K14 complexes formed in either 6 or 9 M urea buffer were separated from uncomplexed K5 and K14 using anion-exchange chromatography, using the same conditions described above. Fractions were collected and analyzed by SDS-PAGE.

Gel Filtration Chromatography

K5, K14, and K5-K14 complexes in either 6 or 9 M urea, 50 mM Tris HCl, 10 mM β-mercaptoethanol, 0.3 mg/ml PMSF buffer, pH 7.4, were subjected to gel filtration chromatography in the presence of molecular weight standards (Sigma Chemical Co., St. Louis, MO). The standards used include rabbit muscle myosin (205 kD), E. coli β-galactosidase (116 kD), BSA (66 kD), and bovine carbonic anhydrase (29 kD). At concentrations of urea >6 M, these proteins behave as denatured monomers (Tsao, 1953; Wong and Tanford, 1973; Chreighton, 1979). Keratins were combined with 75–150 μg of each protein in gel filtration buffer before chromatography.

A Superose 12 column (molecular mass range 1–300 kD; Pharmacia-LKB) was used for gel filtration chromatography of keratin monomers. K5-K14 complexes were sized using a Superose 6 column (molecular mass range 5–5,000 kD; Pharmacia-LKB). Buffer conditions were identical to those used to purify individual keratins (see above). In both cases, the buffer was pumped at a 0.05 ml/min flow rate, 0.1-ml fractions were collected, and elution of proteins was monitored by UV absorbance at 280 μm.
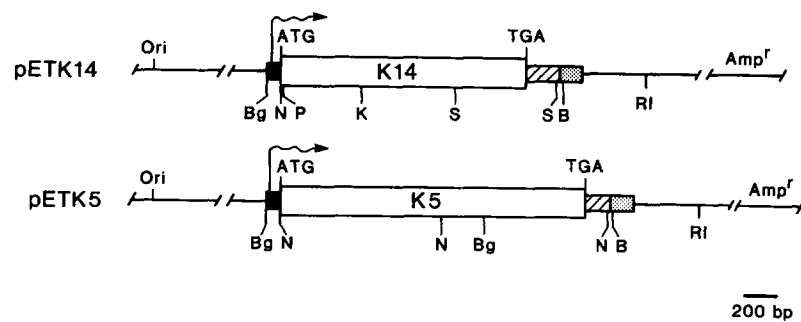

Figure 1. Genetic map of plasmids pETK14 and pETK5. Details of plasmid constructions can be found in Materials and Methods. The components of the plasmid are represented as follows. (a) The black box represents the T7 RNA polymerase promoter used to drive expression of the constructed cDNAs. The transcription initiation site is marked by the arrow. The 5' untranslated sequence is part of the vector, since the K5 and K14 cDNAs were cloned into the Nco I site of pET-8c at the ATG start codon. (b) The white boxes represent complete human K5 and K14 cDNAs, as indicated. (c) The hatched box represents 3' noncoding sequences corresponding to either human K5 or human K14 genes. (d) The stippled box represents the transcription terminator sequence present in the pET-8c expression plasmid. (e) The origin of replication for plasmid pBR322 is indicated (Ori) as is the ampicillin resistance gene contained in plasmid pET-8c. Important restriction endonuclease sites are marked. K, Kpn I; S, Sac I; B, Bam HI; RI, Eco RI; Bg, Bgl II; N, Nco I; P, Pst I.

Chemical Cross-Linking

Glutaraldehyde cross-linking studies were performed in 6 and 9 M urea buffers using a procedure adapted from Quinlan et al. (1986). Samples (125–150 μg/ml) of human vimentin, K14, K5, and K5-K14 were purified by anion exchange chromatography, followed by dialysis for 12 h at room temperature against a solution of 50 mM sodium phosphate, 10 mM β-mercaptoethanol, pH 7.7, containing either 6 or 9 M urea, as indicated in the text. EM-grade glutaraldehyde (Ted Pella, Inc., Irvine, CA) was added such that final concentrations ranged from 0 to 0.12% (vol/vol), and samples were incubated for 30 min at either 10°C (6 M urea) or 15°C (9 M urea). The cross-linking reactions were terminated by addition of one half volume of the same urea buffer, containing 2 M glycine. Cross-linked samples were resolved through 7% SDS polyacrylamide gels, and transferred to nitrocellulose paper by blotting (Towbin et al., 1979). Blots were incubated with either antihuman vimentin (Stellmach and Fuchs, 1989), anti-type I or anti-type II keratin antisera (Fuchs and Marchuk, 1983), followed by ^{125}I-labeled S. aureus protein A (Amersham Corp., Arlington Heights, IL). Blots were then processed for autoradiography using Kodak X-Omat film.

Type I/type II keratin complexes cross-linked in either 6 or 9 M urea were purified by anion exchange chromatography, subjected to gel filtration chromatography, and analyzed by SDS-PAGE as described above. Molecular mass standards were utilized for the 6 M run. For the 9 M run, standards were omitted, but sizes were estimated according to the expected elution profiles for the column.

EM of K5-K14 Complexes and of 10-nm Filaments

Carbon-coated electron microscopic nickel grids (300 mesh; Ted Pella, Inc.) were glow discharged before applying the specimen. K5-K14 complex samples were diluted to 0.01–0.03 mg/ml with urea-Tris buffer, and a 5-μl aliquot was adsorbed on a pretreated grid for 30 s. Grids were then washed gently with several drops of the urea-Tris buffer (30 s), followed by several drops of 10 mM Tris-HCl buffer (1 min), and negatively stained for 30 s with 1% uranyl acetate. Excess stain was removed by blotting with filter paper. Filament preparations were processed in a similar fashion, except that they were diluted to 0.04–0.05 mg/ml with 50 mM Tris buffer and rinsed only with Tris buffer (1 min) before staining. Specimens were examined in

a Philips CM-10 electron microscope operated at an acceleration voltage of 80 kV, under minimal dose conditions. Magnification was calibrated using a #10021 diffraction grating replica from Ernest F. Fulham, Inc. (Schenectady, NY).

Results

Isolation of Bacterially Derived Human Keratins: Purified Keratins Are Fully Competent for IF Assembly In Vitro

Previously, we isolated and characterized near full-length cDNAs encoding the human keratins, K14 (Hanukoglu and Fuchs, 1982) and K5 (Lersch and Fuchs, 1988). Through subsequent isolation and characterization of the functional genes encoding these keratins (Marchuk et al., 1984, 1985; Lersch et al., 1989), we were able to construct full-length cDNAs. To express these cDNAs in bacteria, we subcloned them both individually (pETK14 and pETK5, respectively) into the bacterial expression plasmid pET-8C, which has a T7 RNA polymerase promoter sequence located just 5' from a multiple cloning region (Studier and Moffatt, 1986; Rosenberg et al., 1987). Fig. 1 illustrates the constructs that were engineered.

When E. coli strain BL21(DE3)pLysS, harboring a single copy of the T7 RNA polymerase gene under the control of the IPTG-inducible lacUV5 promoter, was transformed with pETK5 and subsequently treated with IPTG, large cytoplasmic IBs formed that were not present in the untransformed cells. Similar bodies were seen in pETK14-transformed bacteria. That these inclusion bodies contained human keratin was confirmed by immunoelectron microscopy (performed
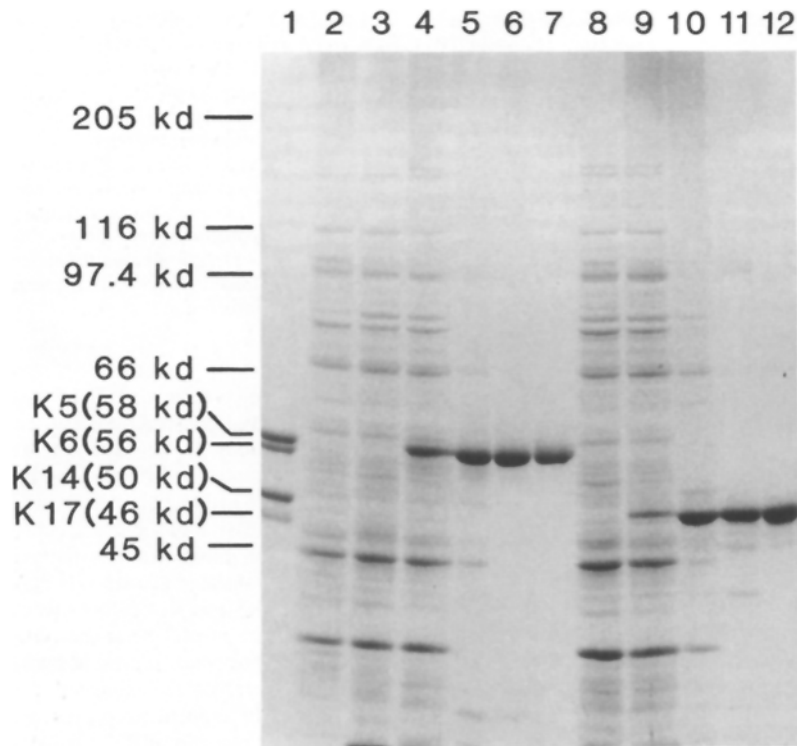

Figure 2. SDS-PAGE analyses of keratin purification. E. coli strain BL21(DE3)pLysS was transformed with pET (control), pETK5-o.f.(out of frame K5 cDNA; control), pETK5, pETK14-o.f.(out of frame K14 cDNA, control); or pETK14, and keratin expression was induced by addition of IPTG to the medium (Studier and Moffatt, 1986). After induction, bacteria were harvested and inclusion bodies were isolated as described in Materials and Methods. Keratins were purified by Mono Q anion exchange chromatography and Superose 12 gel filtration chromatography using an LKB HPLC system (see Materials and Methods). Protein samples from total bacterial protein extracts, inclusion bodies, and from pooled peak fractions of chromatography runs were then analyzed by electrophoresis through 8.5% polyacrylamide SDS gels. Proteins were visualized by staining with Coomassie Blue. Proteins were from (lane 1) IF extract of cultured human epidermal cells (K5$^+$, K6$^+$, K14$^+$, K17$^+$); (lane 2) untransformed BL21-(DE3)pLysS; (lane 3) BL21(DE3)pLysS transformed with pETK5-o.f.; (lane 4) BL21(DE3)-pLysS transformed with pETK5; (lane 5) IBF from bacterial extract in lane 4; (lane 6) Mono Q purification of K5 IBF in lane 5; (lane 7) Superose 12 purification of pooled Mono Q fractions from lane 6; (lane 8) BL21(DE3)pLysS transformed with pETK14-o.f.; (lane 9) BL21(DE3)pLysS trans-

formed with pETK14; (lane 10) IBF from bacterial extract in lane 9; (lane 11) Mono Q purification of K14 IBF in lane 10; and (lane 12) Superose 12 purification of pooled Mono Q fractions from lane 11. Molecular masses of epidermal keratins are indicated at left.
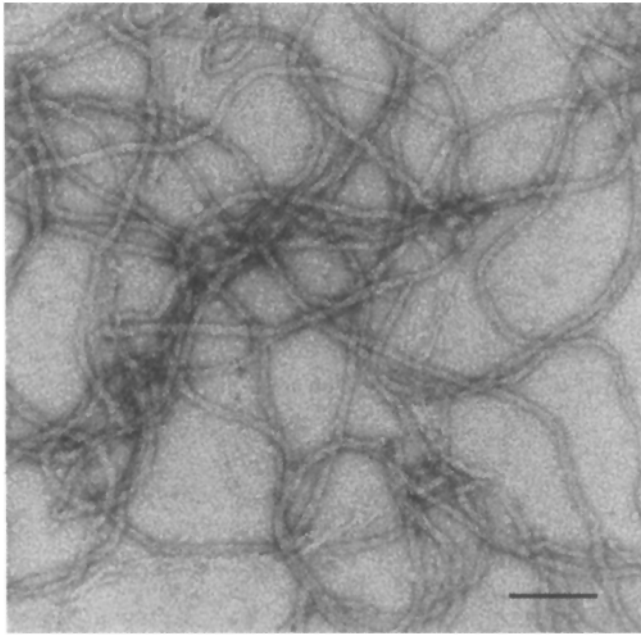
156

Figure 3. In vitro assembly of purified keratins into filaments. Purified K5 and K14 from peak fractions of the Superose 12 column were combined at a concentration of 400 μg/ml in 9 M urea buffer, and dialyzed twice against nonurea buffers as described in Materials and Methods. Assembled filaments were visualized under a Phillips CM 10 electron microscope. Bar, 0.1 μm.

as in Coulombe et al., 1989), using rabbit polyclonal antisera specific for the COOH-terminal domain of either K14 or K5 (not shown).

To further characterize the keratins generated from the pET expression constructs, we first isolated IBFs from pETK5-transformed bacteria, and extracted total proteins from these structures. When resolved by PAGE, the IBF proteins included a prominent 58-kD polypeptide (Fig. 2, lane 5). This band corresponded in electrophoretic mobility to bona fide human K5 from cultured keratinocytes (lane 1). IBF preparations from untransformed bacteria (lane 2) and from *E. coli* transformed with an out-of-frame pETK5 construct (lane 3) yielded protein profiles that were identical to that of the pETK5-transformed cells, with the exception of this single 58-kD band. Subsequent immunoblot analysis using an anti-K5 monospecific antiserum confirmed the identity of the 58-kD band (data not shown). IBF preparations from cells transformed with in-frame constructs of pETK14 produced a 50-kD protein (lane 10), with an electrophoretic mobility identical to that of human epidermal K14 (lane 1). For both keratin-producing bacterial cell lines, ~35–40% of the total inclusion body fraction consisted of keratin. These data are similar to that obtained by Magin et al. (1987), who purified a simple epithelial keratin K8 from transformed *E. coli* bacteria.

Keratins from pETK5- and pETK14-transformed cells were purified to homogeneity in two steps, using ion exchange (FPLC) chromatography, followed by gel filtration (FPLC) chromatography. To maintain keratins as solubilized fractions with uniform and discrete behavior, they were always kept in the presence of at least 6 M urea. Fig. 2 shows the purity of K5 and K14 after (*a*) ion exchange chromatography (lanes 6 and 11, respectively), and (*b*) gel filtration chro-

matography (lanes 7 and 12, respectively). As judged by densitometry scanning of the Coomassie Blue-stained gels, keratins were >98% pure after gel filtration chromatography.

To verify that the purified keratins were competent for filament assembly, we combined K5 and K14 at 0.4 mg/ml in 9 M urea buffer and then dialyzed away the urea as indicated in Materials and Methods. Electron microscopic analysis of the dialyzed mixture demonstrated clearly that some of the *E. coli*-generated proteins were fully competent to form 10-nm filaments (Fig. 3). To determine whether the purified keratins were quantitatively competent for filament formation, we reduced the keratin concentration to as low as 37.5 μg/ml. Even under these conditions, we observed abundant 10-nm filaments. This was initially surprising, since 50 μg/ml had been assigned as the critical concentration, below which keratins purified from mammalian cells did not assemble (Steinert et al., 1976). Hence, not only are our *E. coli*-generated keratins largely, if not wholly, competent for filament formation, but in addition, the critical keratin concentration for filament formation is less than previously measured.

In Separate Solutions of K5 or K14 in 6 M Urea, the Keratins Exist as Monomers

To determine whether purified K5 and K14 alone exist as monomers or in a multimeric state in the presence of 6 M urea and a reducing agent, we repassaged purified keratin preparations through the gel filtration column, this time in the presence of molecular mass standards (Fig. 4). Under these conditions, all the standard proteins were known to exist as monomers (see Materials and Methods). While the standard proteins were not in their native state, their mobility through the gel filtration column was largely as expected, i.e., in proportion to the log of their molecular mass. Relative to these size standards, K5 and K14 eluted at an estimated size of ~55–58 kD and 52–56 kD, respectively (Fig. 4, left and right frames). These size estimations were in good agreement with those predicted on the basis of (*a*) amino acid sequence (Marchuk et al., 1984; Lersch et al., 1989), and (*b*) their electrophoretic mobility through polyacrylamide gels (Sun and Green, 1978). Thus, by these criteria, both K5 and K14 appeared to run as monomers in the presence of 6 M urea and a reducing agent.

To make certain that our assignment of these subunits as monomers was correct, we added 1% SDS to separate urea-β-mercaptoethanol solutions of K5 and K14 and preboiled them. The gel filtration analyses were then repeated in 0.1% SDS urea buffer. The patterns of elution of K5, K14, and all protein standards were indistinguishable from the elution profiles shown in Fig. 4. Since it is well-known from SDS-PAGE analyses that similar conditions lead to quantitative disruption of all keratin–keratin interactions (Sun and Green, 1978; see additional data to follow), and since no difference in elution profiles were observed, we conclude that K5 and K14 by themselves exist as monomers in 6 M urea, 50 mM Tris-HCl, 10 mM β-mercaptoethanol, pH 7.4.

When Combined in the Presence of 6M Urea, K5 and K14 Associate in a 1:1 Ratio to Form a Complex

To determine whether K5 and K14 have the capacity to as-
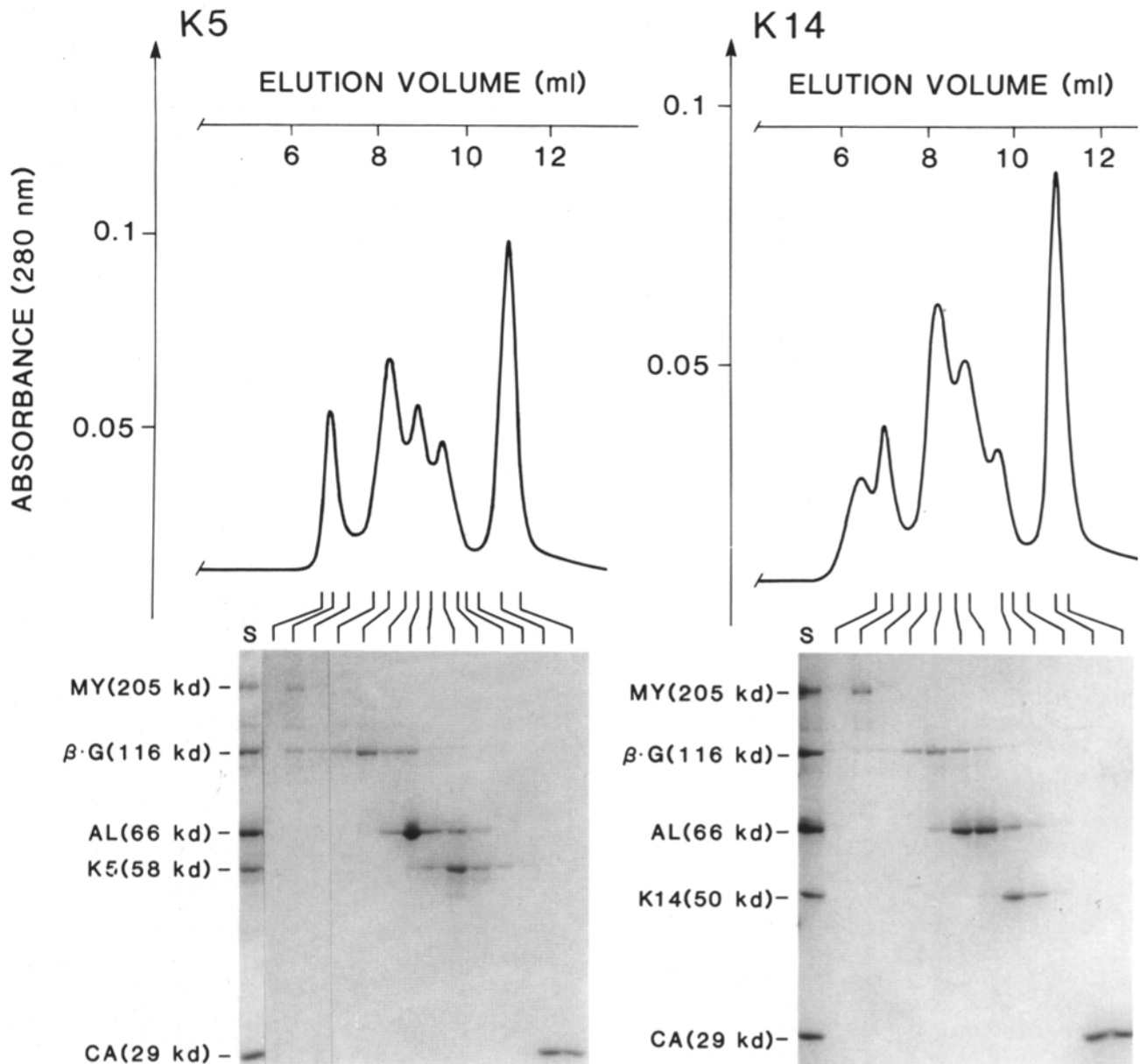
GEL FILTRATION IN 6M UREA

Figure 4. Determination of monomer state of K5 and K14 in 6 M urea. FPLC-purified K5 (left) and K14 (right) were combined with molecular mass standards in 6 M urea buffer and subjected to gel filtration chromatography on Superose 12 as described in Materials and Methods. Protein elution was monitored by ultraviolet absorption at A_{280} nm, and 100-μl fractions were collected. 30-μl aliquots of each fraction were analyzed by electrophoresis through SDS polyacrylamide gels, followed by staining with Coomassie Blue (shown below each UV absorbance profile in the diagram). From left to right, first lane (S) represents an aliquot of protein used in the analysis, and vertical bars over protein profiles indicate sequential fractions examined by SDS-PAGE. Sizes of molecular mass standards are indicated at left. *My*, myosin; *βG*, β-galactosidase; *Al*, BSA; *CA*, carbonic anhydrase.

sociate with each other under conditions where they do not associate with themselves, we combined K5 and K14 in various molar ratios, in the presence of 6 M urea and a reducing agent. Resulting products were examined by (*a*) ion exchange chromatography (Fig. 5), and (*b*) gel filtration chromatography (Fig. 6), both run in the presence of urea and a reducing agent (see Materials and Methods for details). When K5 and K14 were combined in a 2:1 ratio and bound to an anion-

exchange column, two peaks were subsequently eluted: one with 70 mM and one with 133 mM guanidinium hydrochloride (Fig. 5, frame *A*). The first peak eluted at the same salt concentration as pure K5, but the second peak (*arrow*) eluted at a higher salt concentration than either K5 or K14. When aliquots of the peaks were analyzed by SDS-PAGE, the first peak contained pure K5 protein, whereas the second peak contained K5 and K14 in a 1:1 molar ratio, as determined by

K5·K14 COMPLEX FORMATION IN 6M UREA

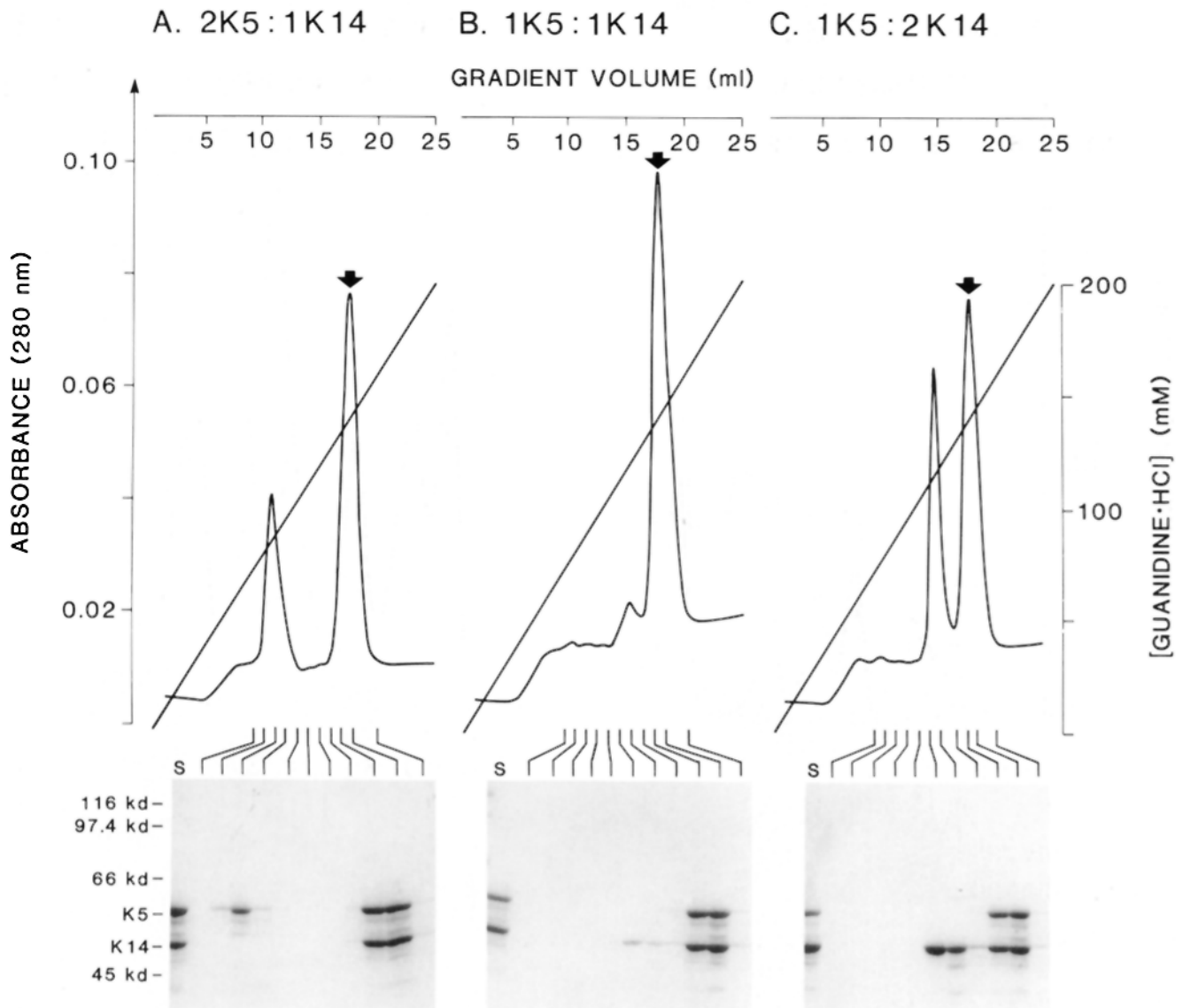## A. 2K5:1K14   B. 1K5:1K14   C. 1K5:2K14

Figure 5. Anion exchange analysis of monomer and heteromer complexes formed upon combining K5 and K14 in 6 M urea. Anion-exchange (Mono Q)-purified K5 and K14 were combined in various ratios, each at a final total keratin concentration of 1.2 mg/ml in 6 M urea buffer and applied to an anion-exchange FPLC column as described in Materials and Methods. Arrow denotes presence of K5:K14 complex. 30-μl aliquots of each fraction were analyzed by electrophoresis through SDS polyacrylamide gels, followed by staining with Coomassie Blue (shown below each UV absorbance profile in the diagram). From left to right, first lane (*S*) represents a 5-μl aliquot of protein used in the analysis and vertical bars over protein profiles indicate sequential fractions examined by SDS-PAGE. Ratios of K5:K14 were (frame *A*) 2K5:1K14; (frame *B*) ~1K5:1K14; and (frame *C*) 1K5:2K14. Sizes of molecular mass standards are indicated at left in daltons. Note presence of faint bands <58 kD represent small amounts of specific degradation products of K5 and K14.

densitometry scanning of the Coomassie Blue-stained gel (frame *A*, gel profile). This 133-mM Gu·HCl peak constituted >95% of the protein when K5 and K14 were combined in ~1:1 molar ratio (Fig. 5, frame *B*). When K5 and K14 were combined in a 1:2 molar ratio, this peak was still observed, but this time it was accompanied by an additional peak eluting with 110 mM Gu·HCl (Fig. 5, frame *C*). SDS-PAGE analysis revealed that this peak contained pure K14, whereas the peak eluting at 133 mM Gu·HCl contained K5 and K14 in a 1:1 molar ratio (frame *C*, gel profile). Collec-

tively, these data indicated that in the presence of 6 M urea and a reducing agent, K5 and K14 associated in an equimolar ratio to form a complex(es) with an as yet unidentified number of K5 and K14 polypeptide chains. Moreover, since none of the three K5/K14 combinations yielded peaks representing *both* unassociated K5 *and* unassociated K14, these data indicate that under the conditions used, the equilibrium greatly favored formation of complexes between K5 and K14.

A priori, the presence of a peak of K5/K14 eluting with a salt concentration greater than either K5 or K14 alone, only

GEL FILTRATION OF K5·K14 COMPLEX IN 6M UREA

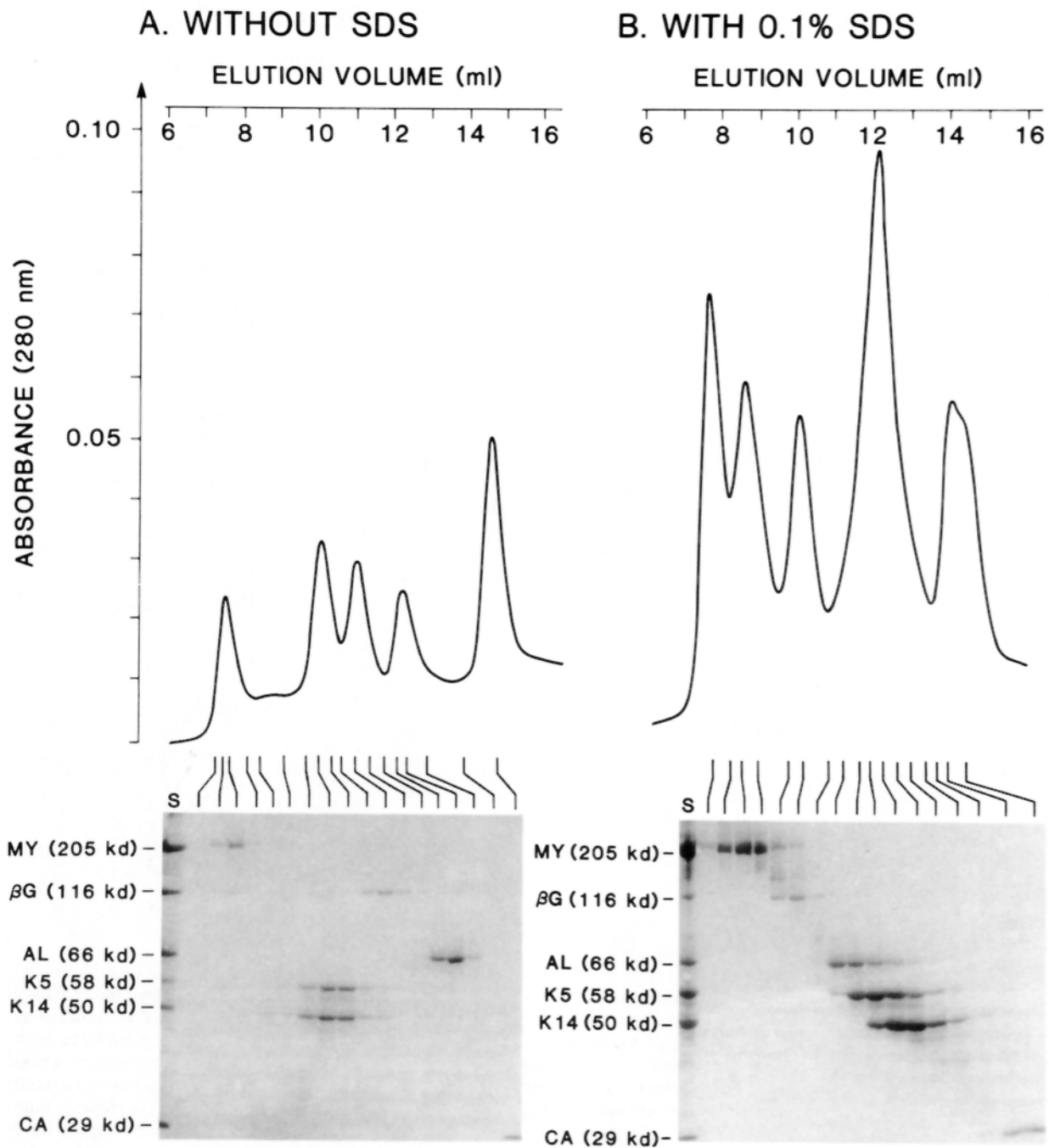## A. WITHOUT SDS

B. WITH 0.1% SDS

Figure 6. Sizing of the K5-K14 complex in 6 M urea by gel filtration. (*A, without SDS*) The K5-K14 complex purified by anion-exchange chromatography was combined with molecular mass standards and applied to a Superose 6 FPLC column. Samples were collected as described in the legend to Fig. 5. 30-μl aliquots of each fraction were analyzed by electrophoresis through SDS polyacrylamide gels, followed by staining with Coomassie Blue (shown below each UV absorbance profile in the diagram). From left to right, the first lane (*S*) represents a 6-μl aliquot of protein used in the analysis, and vertical bars over protein profiles indicate sequential fractions examined by SDS-PAGE. Sizes of molecular mass standards are indicated at left. Note that the complex showed a mobility corresponding to a molecular mass that was larger than that predicted for a dimer, but smaller than that predicted for a tetramer. We later demonstrate that this peak is likely to represent a tetramer, and that the mobility is faster than expected due to the compactness of the complex relative to keratin monomers and other standards. (*B, with 0.1% SDS*) Similar to *A*, but in this case, the complex was treated with SDS and boiled briefly before loading on the Superose 6 column. The running buffer also contained 0.1% SDS. Note that the complex dissociated into monomers, which each eluted according to their respective mobilities.
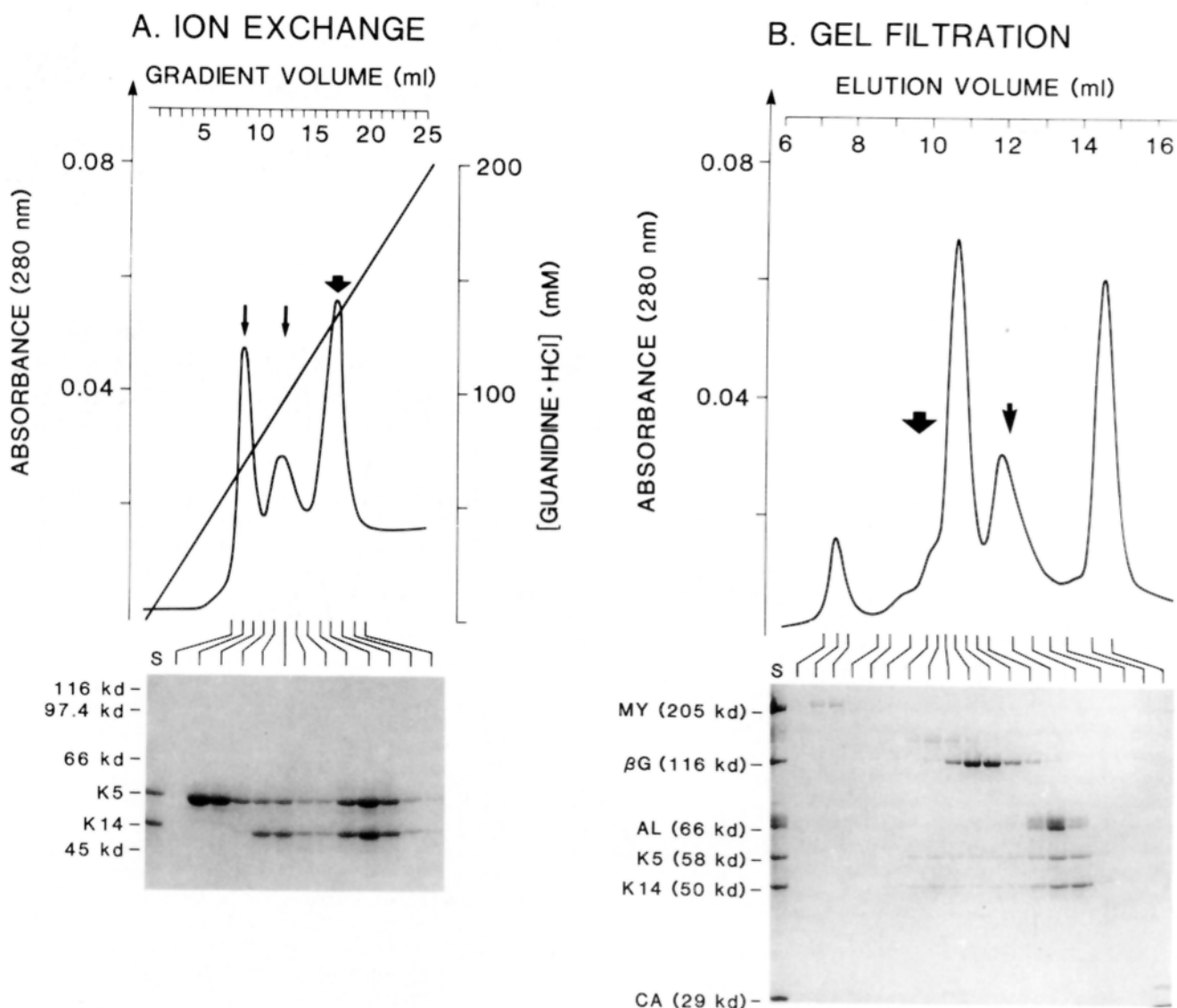
COMPLEX FORMATION IN 9M UREA

A. ION EXCHANGE

B. GEL FILTRATION

Figure 7. Keratin heterodimers exist in 9 M urea. (*A*) Purified samples of K5 and K14 were combined in a 1:1 ratio at a total keratin concentration of 1.2 mg/ml in 9 M urea buffer and applied to a Mono Q anion exchange FPLC column. Thin overhead arrows denote peaks eluting at similar salt concentration expected for K5 (*left*) and K14 (*right*). Thick arrow denotes peak eluting at the same salt concentration as the K5:K14 complex observed in Fig. 6. To verify the composition of peak fractions, 30-μl aliquots were analyzed by electrophoresis through SDS polyacrylamide gels, followed by staining with Coomassie Blue (shown below each UV absorbance profile in the diagram). From left to right, the first lane (*S*) represents an aliquot of protein used in the analysis, and vertical bars over protein profiles indicate sequential fractions examined by SDS-PAGE. Sizes of molecular mass standards are indicated at left. Note: the pure K5 monomer peak showed some trailing, which led to appreciable K5 contamination in the K14 monomer peak. (*B*) Fractions corresponding to the keratin complex were pooled, combined with molecular mass standards, and applied to a Superose 6 FPLC column as described in Materials and Methods. 100-μl fractions were collected and analyzed as described in the legend to Fig. 5. Thick arrow denotes a minor species eluting at the same mobility as that observed for the 6 M urea K5-K14 complex. Thin arrow denotes major species coeluting with serum albumin. Note: This major species eluted before that expected for K5 and K14 monomers, and almost every fraction had a ∼1:1 ratio of K5 and K14 (compare with the behavior of K5 and K14 monomers as shown in Fig. 4, *A* and *B*).

confirmed that K5 and K14 existed as a stable complex under the conditions used. To estimate the size of this complex, we subjected the same mixtures to gel filtration chromatography, along with molecular mass standards (Fig. 6). As shown in frame A for the 1:1 mixture, the complex eluted as a single species, after myosin (205 kD) and before β-galactosidase (116 kD). When based against the monomer molecular mass

standards, the complex showed a mobility with an apparent molecular mass of 135 kD. We anticipated that a K5/K14 complex might elute aberrantly due to (*a*) the extraordinarily tight intermolecular interactions, and (*b*) the relative stiffness of the coiled-coil domain. Hence, further analyses were necessary to determine whether the complex represented a heterodimer (predicted size of 113 kD) (Marchuk et al.,
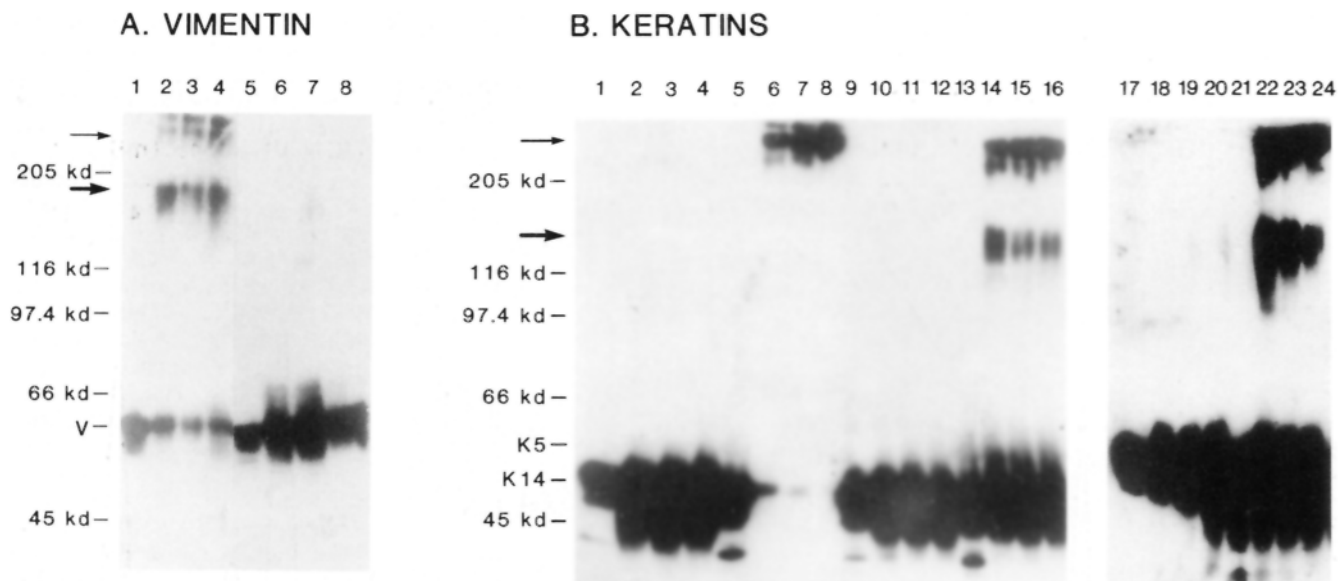
A. VIMENTIN

B. KERATINS

Figure 8. Chemical cross-linking of IF polypeptide chains in the 6 and 9 M urea samples. (*A*) Since the properties of glutaraldehyde cross-linked, vimentin homodimers were known (Quinlan et al., 1986), vimentin was used as a control. Details of the *E. coli* expression vector construct used to generate human vimentin will be published elsewhere (M. B. McCormick and E. Fuchs). Human vimentin was purified using FPLC anion exchange chromatography as described for keratins. Cross-linking studies on purified vimentin were carried out in the presence of either 6 M (lanes *1-4*) or 9 M urea (lanes *5-8*) sodium phosphate buffer as described in Materials and Methods. Samples shown were cross-linked in the presence of the following glutaraldehyde concentrations (vol/vol) (lanes *1* and *5*) 0%; (lane *6*) 0.02%; (lanes *2* and *7*) 0.04%; (lanes *3* and *8*) 0.08%; and (lane *4*) 0.12%. Mobilities of molecular mass standards are shown at left. Mobility of vimentin monomer is indicated as *V*. Thick arrow indicates mobility of the vimentin homodimer (consistent with that reported by Quinlan et al., 1986); thin arrow indicated mobility of putative vimentin homotetramers. Note: a small amount of cross-linked vimentin did not enter the gel. (*B*) Human K5 and K14 were purified alone or as a complex using FPLC anion exchange chromatography, and cross-linking studies on K14 alone (lanes *1-4* and *9-12*), K5 alone (lanes *17-20*), or the K14-K5 complexes (lanes *5-8, 13-16*, and *21-24*) were carried out in the presence of either 6 M (lanes *1-8*) or 9 M urea (lanes *9-24*) phosphate buffer as described in Materials and Methods. Blots were incubated with antitype I keratin (lanes *1-16*) or anti-type II keratin (lanes *17-24*) (Fuchs and Marchuk, 1983), followed by ^{125}I-labeled *S. aureus* protein A. Samples shown were cross-linked in the presence of the following glutaraldehyde concentrations (vol/vol) (lanes *1, 5, 9, 13, 17*, and *21*) 0%; (lanes *10, 14, 18*, and *22*) 0.02%; (lanes *2, 6, 11, 15, 19*, and *23*) 0.04%; (lanes *3, 7, 12, 16, 20*, and *24*) 0.08%; and (lanes *4* and *8*) 0.12%. Mobilities of molecular mass standards are shown at left. Mobility of keratin monomers are indicated as K5 and K14. Thick arrow indicates mobility of the keratin heterodimer; thin arrow indicates mobility of keratin heterotetramers. Notes:(*a*) overexposures of the gels were used to demonstrate the absence of any other bands. (*b*) There was no cross-linking observed when K5 was subjected to glutaraldehyde in either 9 M urea (shown) or 6 M urea (not shown). (*c*) That the cross-linked dimers and tetramers contained a 1:1 ratio of K5 and K14 was confirmed by measuring the amount of radiolabel in the dimer and tetramer bands of the anti-type I and anti-type II blots with the amount of radiolabel obtained by dotblotting a series of known concentrations of K14 and K5 in parallel.

1984; Lersch et al., 1989) or a heterotetramer (predicted size of 226 kD). However, since the single heteromeric complex showed no evidence of dissociation during the run, it was already apparent that the intermolecular interactions leading to its formation must have been particularly strong.

The 1:1 complex of K5 and K14 formed in the presence of 6 M urea was readily dissociated by boiling the sample in the presence of added 1% SDS, as judged by gel filtration chromatography of the boiled mixture. Under these conditions, K5 and K14 monomer peaks were obtained (frame *B*), both appearing after the albumin peak, and eluting according to their predicted molecular mass. These data confirm that (*a*) the aberrant elution of the K5:K14 peak in the absence of SDS was due to the nature of the complex formed, and (*b*) K5 and K14 behave independently when coexisting in a 6 M urea solution containing SDS.

A Smaller Complex of K5 and K14 Exists in 9 M Urea: Indications of Heterodimer Formation

Since our studies of combined K5 and K14 in 6 M urea re-

vealed the existence of extraordinarily stable complexes with no detectable monomer pools, we wondered whether we might be able to find conditions that would enable us to further dissociate the complex, and possibly dissect its composition. To accomplish this, we progressively increased the concentration of urea used in our combination assays up to 9 M. Remarkably, even at 9 M urea, a 1:1 mixture of K5 and K14 produced a complex eluting at 133 mM GuHCl on anion exchange chromatography (Fig. 7, frame *A: thick arrow*). However, in contrast to our previous anion exchange chromatography data, an appreciable amount of keratin eluting at salt concentrations characteristic of both K14 and K5 monomers were detected in the 9 M urea runs (*smaller arrows*). Hence in 9 M urea, there must be an equilibrium between monomers and complex(es).

When the complex was analyzed by gel filtration chromatography, it eluted as two species (frame *B*). SDS-PAGE analysis of the column fractions revealed that both species contained roughly equal amounts of K5 and K14 protein. One of these species eluted after myosin, but before β-galac-
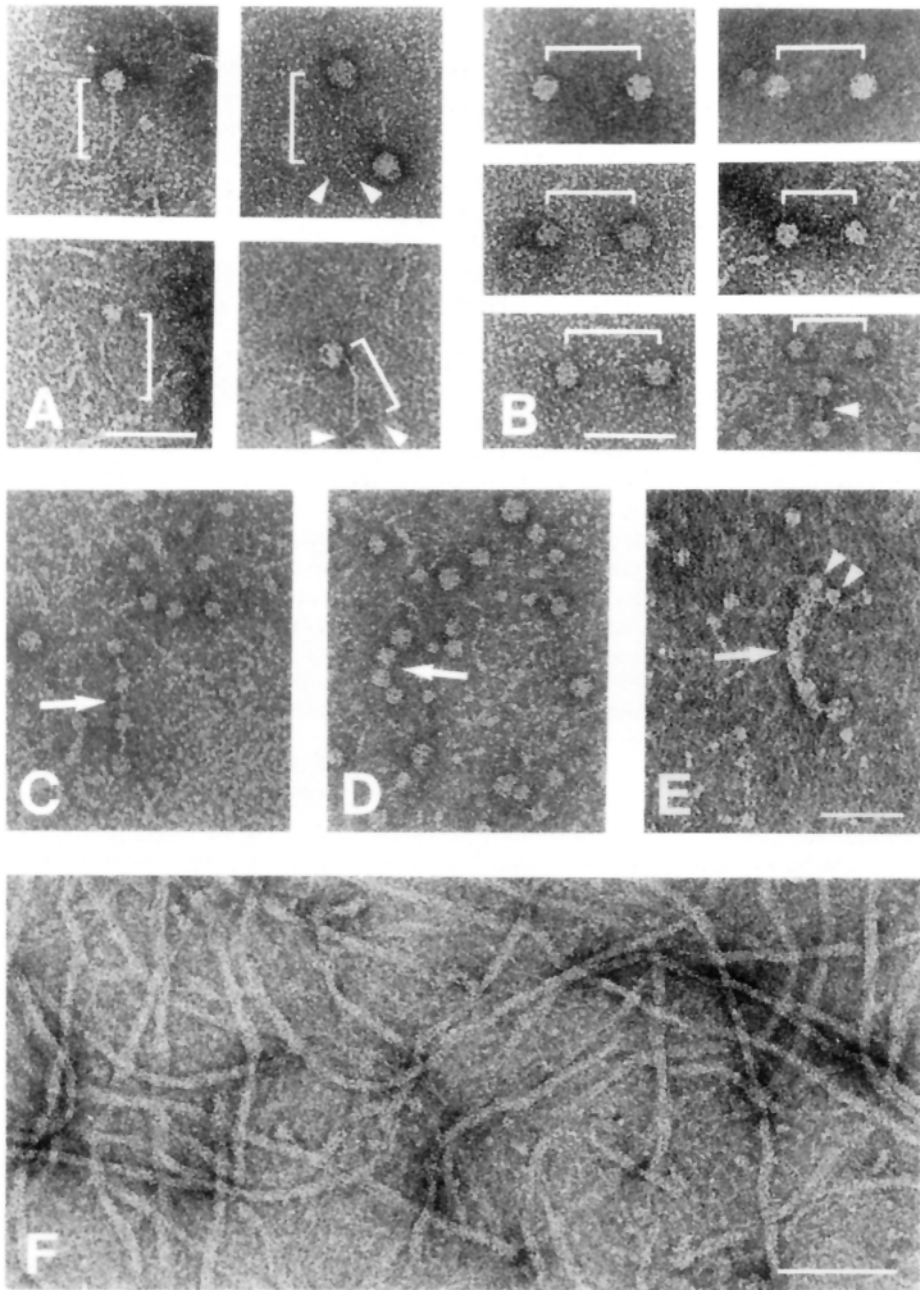
Figure 9. Electron microscopic visualization of keratin heterodimers and heterotetramers. K5 and K14 complexes formed in either 6 or 9 M urea were purified by anion-exchange chromatography and subjected to negative staining and EM as described in Materials and Methods. Part of the 9 M urea sample was dialyzed against 4 M urea. (Frames in *A*) The structures prevalent in the 9 M urea sample and identified as a K5-K14 heterodimer. Note the lollipop-like structures, with a rod-shaped domain of 45-50 nm, indicative of two coiled-coil polypeptide chains aligned in parallel and in register. Arrowheads point to the nonglobular tail domains visible for some dimers. (Frames in *B*) The structures prevalent in the 6 M urea sample, but also seen less frequently in 9 M urea. The structure, identified as a K5-K14 heterotetramer, has a dumb-bell-like shape indicative of two antiparallel dimers, aligned in register. Note: generally, the tetramers showed rod domains of 45-50 nm, while sometimes the length was less than this (see the tetramers denoted by arrowheads). In these cases, the rod was often thicker. (Frames *C-E*) Structures seen in 4 M urea. The structure in *C* appears to involve end-to-end associations of tetramers, leading to protofilament-like fibers. The structure in *D* appears to involve lateral interactions of tetramers, and are similar to what might be expected from a half-staggered conformation of two heterotetramers. The structure in *E* seems to be a partially assembled keratin filament-like structure. (Frame *F*) Filaments reconstituted from dialysis of heterotetramer complexes made in the presence of 6 M urea. Note: filaments could also be reconstituted from dialysis of heterodimer complexes formed in 9 M urea. Bars: (*A*, *B*, and *E*) 50 nm, bar in *E* applies to frames *C-E*; (*F*) 100 nm.

tosidase, i.e., as did the entire complex formed in 6 M urea. The second species coeluted with albumin, i.e., with a predicted size of approximately half that seen for the 6 M urea complex. Hence both species showed aberrant mobility through the gel matrix, and yet both eluted ahead of the predicted mobilities of the K5 and K14 monomers (compare Fig. 4, *A* and *B*, with Fig. 7 *B*). These data suggested that in 9M urea, the smaller keratin complex, eluting aberrantly with a molecular mass characteristic of an ∿70 kD random coil, was a heterodimer. In 9 and 6 M urea, the larger keratin complex, eluting with a molecular mass characteristic of an ∿135 kD random coil, must then be a heterotetramer. The apparent trailing of protein complexes between the two ma-

jor species in 9 M urea (Fig. 7 *B*) suggests that a greater amount of putative tetramer may have actually been present in the anion exchange column-purified sample, and this may have partially dissociated during the dilution of the gel filtration run. Additional data below support this notion.

Chemical Cross-Linking Verifies the Existence of Keratin Heterodimers and Heterotetramers

To verify that our assignments of the 6 M heterotetramer and the 9 M heterodimer were correct, we subjected the complexes to chemical cross-linking with glutaraldehyde. As a reference, we also cross-linked human vimentin in the presence of 6 M urea, since under similar denaturing conditions,

vimentin is known to exist mostly as a homodimer (Quinlan et al., 1986). On SDS polyacrylamide gels, the cross-linked vimentin homodimer is known to migrate aberrantly with an apparent size of 170–200 kD (Quinlan et al., 1986). When we resolved our cross-linked human vimentin by SDS-PAGE, followed by immunoblot analyses and autoradiography, we observed a major species migrating at ∼175 kD, with a minor species at >240 kD (Fig. 8 A, lanes 1–4). At 9 M urea, no cross-linking was obtained with vimentin (lanes 5–8). These data are in good agreement with those obtained by Quinlan et al. (1986), and indicated that the ∼175-kd complex represented the homodimer, and the >240-kD complex represented the homotetramer.

In contrast to vimentin, when K14 and K5 were placed separately in 6 or 9 M urea and exposed to increasing concentrations of glutaraldehyde, neither keratin alone showed any evidence of cross-linking (Fig. 8 B, K14, lanes 1–4, 6 M urea; lanes 9–12, 9 M urea and K5, lanes 17–20, 9 M urea). In contrast, the mixture of K14 and K5 in 6 M urea showed appreciable cross-linking, even at relatively low concentrations of glutaraldehyde (Fig. 8 B, lanes 5–8; anti-K14 immunoblot shown; anti-K5 immunoblot analogous, but not shown). The electrophoretic mobility of the complex was >220 kD, and as expected, it was detected by immunoblot analysis with antisera against both type I and II keratins. The fact that the complex migrated with slower mobility than the vimentin dimer, and yet the actual mass of each keratin is less than that of vimentin, indicated that the cross-linked keratin complex was a heterotetramer. This conclusion was further strengthened when we repeated our gel filtration analyses, this time with the cross-linked keratin (not shown): relative to the random coil standards, the cross-linked complex eluted as if it were a 135-kD species (i.e., a similar gel filtration profile to that in Fig. 6 A), but when the peak fractions were analyzed by SDS-PAGE, the cross-linked complex ran as a >220-kD species, rather than a 58-kD and 50-kD species. Collectively, these data confirmed our assignment of the 135-kD gel filtration species as the heterotetramer and demonstrate that the heterotetramer runs aberrantly relative to fully denatured proteins in urea gel filtration chromatography.

When K5 and K14 were subjected to glutaraldehyde in the presence of 9 M urea, they formed two heteromeric complexes, one with a mobility of >220 kD and one which was much smaller (∼150 kD) (Fig. 8 B, lanes 13–16 and 21–24). Both complexes were present as a 1:1 mixture of K5 and K14 as judged by immunoblot analysis with anti-K14 (lanes 13–16) and anti-K5 (lanes 21–24). Since the >220-kD species is a tetramer, the smaller ∼150-kD SDS-PAGE species must be a heterodimer. This conclusion was confirmed by gel filtration analyses of the 9 M cross-linked species: according to random coil standards, the >220-kD species eluted as if it were a ∼135-kD random coil, and the 150-kD species eluted as if it were a ∼70 kD random coil (data not shown). Our findings are in good agreement with our gel filtration studies of uncross-linked keratin complexes, and demonstrate unequivocally that in 6 M urea, K5 and K14 exist as stable tetramers, while in 9 M urea, K5 and K14 exist as a mixture of heterodimers, heterotetramers, and monomers. Moreover, the abundance of cross-linked heterotetramers in 9 M urea are in agreement with the notion that the trailing of the tetramer observed in the gel filtration was due to dissociation of the heterotetramer into heterodimers during the run.

The Structure of Keratin Heterodimers, Heterotetramers, and Higher Ordered Structures

Using EM, we examined the structure of our fractions of monomers and heteromeric complexes. While high-resolution low angle rotary shadowing was not feasible due to the presence of urea in our buffers, negative staining enabled visualization of the subunits. K5 and K14 monomers had no discernible structure, at least within the limits of resolution offered by negative staining (not shown). In contrast to the structure of keratin monomers, heterodimers in 9 M urea showed a lollipop-like structure, with a prominent globular domain at one end (Fig. 9 A). The overall structure was similar to that seen for dimers of lamin IF subunits, where two polypeptide chains appear to be aligned in parallel and in register (Aebi et al., 1986, 1988; Parry et al., 1987). The rod domains of the dimers shown are ∼45–50 nm, consistent with the length of a 310 amino acid residue coiled-coil (see Aebi et al., 1986, 1988; Parry et al., 1987). In some cases, the other nonhelical end of each keratin in the heterodimer could also be seen (see arrowheads in A). Since the amino terminal ends of K5 and K14 are larger than their carboxy ends, it seems most likely that the globular end of the dimer represents the amino ends of the two keratins. Although we cannot exclude the possibility that the enlarged "head" domain arises from a negative staining artifact (i.e., excessive exclusion of negative stain), we think that its size most likely reflects the random coil nature of the globular amino domain in urea (Steinert et al., 1983, 1984). The heterodimer structure thus seems to consist of K5 and K14 polypeptides aligned in register and in a parallel fashion, a notion which is consistent with previous predictions based on (a) model building and Fourier transform analyses and (b) biochemical analyses of proteolytic fragments of keratins isolated from partial enzymatic digestion of keratin filaments (McLachlan, 1978; Crewther et al., 1983; Woods and Inglis, 1984; Parry et al., 1985, 1987).

In 9 M urea, occasional dumb-bell-like structures were seen, and at lower urea concentrations, the number of these structures increased significantly (Fig. 9 B). While the rod domains were sometimes difficult to see, the spacing between globular domains was often 45–50 nm. These dumb-bell structures were reminiscent of those obtained by Geisler et al. (1985), who examined tetramers of headless/tailless desmin rods decorated with an antibody against the COOH-terminal portion of the rod. For intact keratin heterotetramers, the putative non-helical amino end domain was sufficiently large under the strongly denaturing conditions used, so that no antibody was necessary to create the dumb-bell-like structure. Our data demonstrate that similar to desmin, the keratin heterotetramer often consists of two heterodimers, aligned in an antiparallel fashion and seemingly in register.

Interestingly, we noticed that some dumb-bell structures had rod domains that were only ∼30–40 nm (see examples denoted by arrowheads in Fig. 9 B). It is possible that under the strongly denaturing conditions used here, the coiled-coil might be in equilibrium with a partially denatured conformation. Alternatively, the coiled-coil rod could be in equilibrium with a more compacted structure, a notion consistent with our observations that (a) the shorter rods often appeared somewhat thicker than the 50-nm long version; and (b) these compacted rods were also seen under less stringent condi-

tions (see below). However, we cannot rule out the possibility that these structures arise from two antiparallel dimers that are partially staggered, as proposed for the tetramers in the paracrystalline structures of glial filament protein (Stewart et al., 1989; see also Fraser et al., 1987; Aebi et al., 1988). Further studies will be necessary to distinguish between these possibilities.

We were interested to know what keratin structures might exist at concentrations of urea <6 M, because when we had attempted to fractionate 4 M urea complexes by gel filtration chromatography, no discrete peaks were obtained (not shown). As suspected, a mixture of higher ordered structures were present in addition to dimers and tetramers (Figs. 9, C–E). Among these included structures which appeared to be strings of tetramers, linked end to end (Fig. 9 C), and occasionally structures which resembled two tetramers arranged in a half-staggered conformation and packed laterally (Fig. 9 D). In addition, even higher ordered structures composed of a larger number of keratin subunits were seen (Fig. 9 E). Since no one structure prevailed, we could not ascertain whether any of these structures were likely to be bona fide intermediates in the assembly process. These data underscore our findings that many of the interactions leading to higher ordered filament assembly appear to take place simultaneously in parallel, rather than sequentially in series.

Keratin Heterodimers and Heterotetramers Are Competent for Filament Formation

A priori, the isolation of heterodimers and heterotetramers of K5 and K14 did not necessarily mean that these structures were competent for filament formation. To examine whether these subunits are viable precursors for filament formation, and not merely dead-end structures, we dialyzed purified complexes in 6 and 9 M urea as described in Materials and Methods, and examined the resulting structures under the electron microscope. Our results indicate that whether we began with purified complexes formed in the presence of 9 or 6 M urea, bona fide 10-nm filaments assembled (Fig. 9 F, dialysis from 6 M urea). Moreover, based upon protein concentration and the number of filaments formed upon dialysis of these, it was evident that filament formation occurred with an efficiency comparable to that seen when K5 and K14 monomers in 9 M urea were combined without purification of the heteromeric complexes, and subsequently subjected to dialysis. Since the heteromers were the only small subunit complexes which we detected, and since 10-nm filaments could be obtained with high efficiency upon dialysis of the urea buffers, it seems likely that the heterodimers and heterotetramers we have isolated are the building blocks of keratin filaments.

Discussion

The Dimer

Many of the initial predictions of keratin dimer subunit composition and structure came from studies on other IF proteins. Among the most elegant of these studies include recent investigations of the nuclear lamin dimers, where rotary shadowing and electron microscopy have enabled visualization of the polypeptide chains in parallel and in register (Aebi et al., 1986; Parry et al., 1987). In addition, Quinlan

et al. (1986) purified desmin, vimentin, and neurofilament dimers by HPLC in 3 M guanidinium hydrochloride. The dimer state of these subunits was confirmed by chemical cross-linking and analytical ultracentrifugation studies. Electron microscopic examination of the dimer fractions indicated that the coiled-coil rod was ~40–45 nm long and ~2–4 nm in diameter (Quinlan et al., 1986). Hence, on the basis of other IF proteins alone, it could be predicted that the characteristic structure of the coiled-coil of keratin IFs would be a dimer, arranged in parallel and in register.

Since these pioneering studies on the basic structure of the IF coiled-coil, there has been little dispute over the putative dimer structure for keratins. However, whether these dimers exist as heterodimers, homodimers, or both has been a matter of considerable controversy (Gruen and Woods, 1983; Woods and Inglis, 1984; Parry et al., 1985; Eichner et al., 1986; Quinlan et al., 1984, 1986; Hatzfeld et al., 1987; Hatzfeld and Weber, 1990). The issue is an important one, because given the antiparallel nature of the tetramer, homodimers would lead to tetramers with polarity, whereas heterodimers would lead to tetramers with no polarity. Our ability to isolate heterodimers of K5 and K14 under conditions where K5 or K14 by themselves exist as monomers provided unequivocal proof that type II and type I keratins can associate as heterodimers. This conclusion was reached independently in a recent study by Hatzfeld and Weber (1990), where cross-linking of a genetically engineered cysteine residue in the rod domain of K8 and K18 was used to isolate the heterodimer. In our studies of wild-type epidermal keratins, the ability of the heterodimer to persist in the presence of 9 M urea and without any covalent cross-linking of the two polypeptide chains is truly remarkable, and indicates that the intermolecular associations of K5 and K14 are among the strongest noncovalent interactions that exist in nature. In fact, this extraordinary stability of the coiled-coil heterodimer, coupled with its aberrant behavior, i.e., compact in gel filtration and expanded when cross-linked and subjected to SDS-PAGE, explains why the existence of the heterodimer has been so difficult to demonstrate.

Using native gel electrophoresis (not shown), gel filtration chromatography in 4 M urea, and chemical cross-linking in 6 M urea, we were never able to detect the existence of K5 and K14 homodimers, a structure purported to exist, at least for K8 and K18 (Quinlan et al., 1986; Hatzfeld et al., 1987; Hatzfeld and Weber, 1990). While we did detect nonspecific aggregation of keratin monomers at concentrations of urea <6 M, we never obtained convincing evidence for any appreciable pool of specific coiled-coil homodimers. Since heterodimer associations are not only extraordinarily stable, but also fully competent to assemble into 10-nm filaments in vitro, it seems unlikely that homodimers could play a comparable role in the assembly process. Not only would the coiled-coil interactions of homodimers be distinct from those of the heterodimer, but in addition, the associations that lead to heterotetramer and higher ordered structures would also be largely different. Thus, we conclude that keratin heterodimers are the most likely candidates for the coiled-coil structure of epidermal IFs in vivo as well as in vitro.

Our finding that heterodimers of K5 and K14 exist even in the presence of 9 M urea and 10 mM β-mercaptoethanol underscores an unusually strong association between two poly-

peptide chains that share only 29% sequence identity within their 310 amino acid residue coiled-coil domains. Understanding the molecular forces promoting these potent interactions will be limited so long as crystallization of the coiled-coil remains elusive. However, in the absence of such information, our ability to isolate, identify, and characterize keratin heterodimers has provided us with a foundation for future model building and for interpreting the effects of site-directed mutations on dimer formation and stability. Inspection of the sequences within the coiled-coil domains of K5 and K14 already indicate that in addition to hydrophobic interactions within the heptad repeat, ionic interactions may also play a role in stabilizing the dimer. In fact, ~30% of all residues within these coiled-coil domains are charged amino acids (Hanukoglu and Fuchs, 1982; Marchuk et al., 1984; Lersch and Fuchs, 1988; Lersch et al., 1989).

That ionic interactions might be important in promoting coiled-coil formation has been suggested previously by McLachlan and Stewart (1975), who noted in the course of Fourier transform analyses and model building that there is a periodic distribution of charged side-chains in α-tropomyosin. Fourier transform analyses of partial segments of the coiled-coil domains of type I and type II wool keratins has also revealed a periodicity of alternating bands of positively and negatively charged residues, which could play a role in stabilizing a coiled-coil if the keratins were aligned in a parallel fashion (Parry et al., 1977; McLachlan, 1978; McLachlan and Stewart, 1982; Conway and Parry, 1988). For K5 and K14, there are 57 residues throughout the coiled-coil domain that are both charged and conserved. Half of these are in positions e or g of the heptad, i.e., two positions flanking the hydrophobic residues (a and d). The precise role that these residues might play in dimer stabilization remains to be elucidated.

The Tetramer and Beyond: A Model for Intermediate Filament Assembly

While chemical cross-linking studies have long postulated the existence and composition of keratin heterotetramers, some controversy has remained concerning the arrangement of keratin and other IF polypeptide chains within the subunit. For isolated rod domains of desmin, an antibody decorating the COOH-terminal portion of the coiled-coil created 50-nm long dumb-bell-like structures as visualized by EM (Geisler et al., 1985; see also Ip et al., 1985). Our data provided the first opportunity to visualize undecorated and intact IF tetramers of antiparallel dimers, and confirm earlier studies which had suggested that tetramers consist of dimers arranged in an antiparallel fashion.

Our finding that at least a portion of the tetramers had rod domains of ~50 nm was consistent with previous analyses of keratin tetramers (Quinlan et al., 1984). Moreover, even the 30–40-nm dumb-bell-like structures which we obtained under strongly denaturing conditions could be interpreted as being unstaggered, antiparallel dimers, either existing in a partially denatured state or in a compacted state. Despite our finding that IF keratin tetramers exist in a largely unstaggered, antiparallel fashion, we could not rule out the possibility that the 30–40 nm tetramers observed in 6 M urea represent antiparallel dimers in a partially staggered configuration. A staggered tetramer conformation is consistent with model building (Crewther et al., 1983; Fraser et al.,

1986) and analysis of paracrystal formation of IFs (Parry et al., 1987; Stewart et al., 1989), showing that antiparallel dimers might be able to organize in a partially-staggered configuration. Aebi et al. (1988) has suggested that if both staggered and unstaggered tetramers occur, there might be an equilibrium between the two forms, leading to "tetramer switching." While our data on K5 and K14 don't resolve this issue, the existence of a dynamic equilibrium between two tetramer forms both competent for IF assembly seems unlikely in light of (a) the extraordinary stability of the intermolecular interactions leading to tetramer formation; and (b) the complex hierarchy of interactions involved in packing of subunits and the assembly of the 10-nm filament.

To date, we have not yet found conditions that will provide us with homogeneous populations of larger subunit structures. However, the coexistence of monomers, dimers, and even tetramers in the presence of 9 M urea and a reducing agent suggests that a number of defined associations among keratins may take place in parallel, rather than in series, and that the keratin filament assembly process might not occur by a linear sequence of events. This notion is consistent with our detection of a variety of different structures in 4 M urea, including apparent protofilament-like strings of tetramers, linked end-to-end as well as possible octamer-like structures indicative of lateral packing of tetramers. In the future, it may be possible to find suitable conditions to examine these higher-ordered structures by creating mutant subunits which selectively prevent one type of interaction but not others.

Despite the fact that pure populations of octamers have not been isolated, nor does it seem likely that significant pools of octamers will be found in vivo, their existence has been postulated as the building block of protofibrils, the 4.5-nm fibers that intertwine laterally to give rise to the overall 10-nm diameter of the IF (Aebi et al., 1983; Quinlan et al., 1984; Ip et al., 1985; Eichner et al., 1986; Geisler et al., 1986). Scanning transmission EM data have yielded a mass per unit length of the keratin filament that is consistent with the existence of (a) 4 protofibrils per full 10-nm width of the filament, and (b) protofibrils composed of eight polypeptide chains packed laterally to give rise to the 4.5-nm diameter (Steven et al., 1983; Engel et al., 1985). An octameric structure composed of two tetramers arranged in a half-staggered configuration would not only account for the lateral width of the protofibrils in IFs, but it would also account for the 22–25-nm axial repeat of IFs that is visualized by electron microscopy (Milam and Erikson, 1982; Henderson et al., 1982; Aebi et al., 1983, 1986; Ip et al., 1985; Coulombe and Fuchs, unpublished observations). Indeed, as pointed out by Aebi et al. (1988), in order to explain this axial repeat, a staggering of tetramers should take place if the tetramers themselves are unstaggered. The presence of structures such as the one shown in Fig. 9, frame D is suggestive that such lateral packing does take place during filament formation. Hence, while the simultaneous occurrence of end-to-end interactions might preclude the existence of a substantial pool of staggered octamers, our data are in agreement with the notion that staggered tetramer packing may occur during filament assembly. Collectively, our data suggest a model for the generation of the building blocks for keratin filament assembly (Fig. 10 A).

Understanding how tetramers and possibly higher ordered subunit structures associate into protofilaments and proto-

A. Formation of Heteromeric Subunits
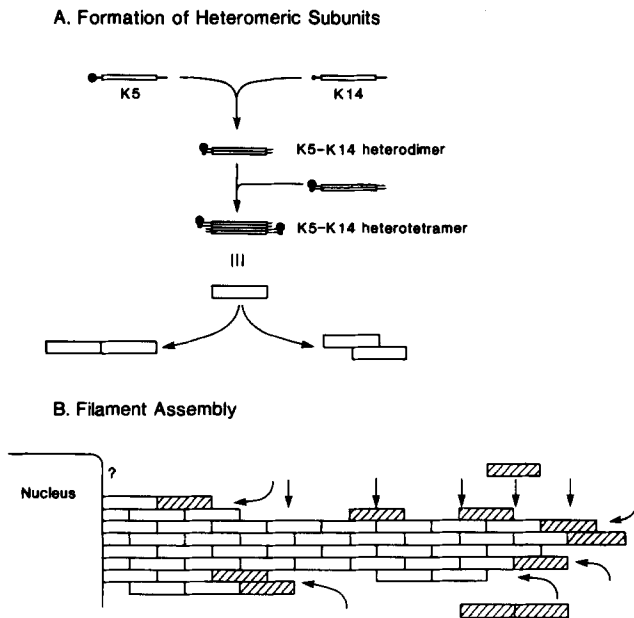

B. Filament Assembly

Figure 10. Model for keratin filament assembly. (*A*) Formation of heteromeric subunits. This part is based on (*a*) our isolation and characterization of heterodimers as the most stable multimeric form; (*b*) production of heterotetramers when denaturing conditions were made less stringent; (*c*) largely unstaggered configuration of lollipop and many dumb-bell-like structures, as judged by EM; and (*d*) the necessity that lateral packing of tetramers must occur in a staggered fashion if tetramers themselves are unstaggered, to account for the 21-25 nm axial repeat (as discussed, some of our data could reflect antiparallel dimers in a partially staggered state, and if so, tetrameric staggering may be less than that shown). The rod of K5 and K14 corresponds to the 310 amino acid domain, which is largely α-helical, and which contains the heptad repeat of hydrophobic residues indicative of a coiled-coil. The globular domain represents the amino terminal nonhelical segments of K5 and K14, which are 168 residues, and 115 residues, respectively, and which are the most likely candidates for the globular portion of the lollipop and dumb-bell structures. The thin tail represents the carboxy terminal nonhelical segments of K5 and K14, which are 109 and 46 residues, respectively. The model suggests that both end-to-end associations and lateral associations of tetramers can occur simultaneously, in agreement with the structures observed in 4 M urea (frames 9, *C* and *D*, respectively). (*B*) Filament assembly. This part is based on (*a*) normal and scanning transmission electron microscopic data indicating that four protofibrils constitute the full 10-nm diameter of the keratin filament and that each protofibril comprises ~8 polypeptide chains per diameter width (Aebi et al., 1983; Steven et al., 1983; Quinlan et al., 1984; Engel et al., 1985); (*b*) immunofluorescence examination of a tagged K14 keratin expressed in epithelial cells, at early times after transfection (Albers and Fuchs, 1987), indicating that newly synthesized keratin is incorporated relatively uniformly throughout the existing keratin filament network (see also Vikstrom et al., 1989; Ngai et al., 1990); (*c*) in vivo filament recovery studies of epithelial cells whose endogenous keratin filament network was temporarily obliterated by transient expression of a COOH-terminal mutant keratin (Albers and Fuchs, 1987): one possible interpretation of these studies is that de novo keratin filament formation may preferentially occur at the nuclear surface and grow towards the cytoplasmic membrane (see also Eckert et al., 1982; Georgatos and Blobel, 1987), although this has not been unequivocally demonstrated (the question mark indicates the present uncertainty of this point); (*d*) scanning transmission

fibrils, respectively and how these smaller fibers interact laterally to give rise to the 10-nm filament must await further molecular probing into the complex structure of the intermediate filament. Recently, however, gene transfection studies on wild-type and mutant epidermal keratins have provided some insights into the hierarchy of the IF assembly process (Albers and Fuchs, 1987, 1989). When expressed in cultured epithelial cells, K14 integrated into the preexisting keratin filament network, and even at early times after transfection, a tagged keratin was distributed evenly throughout the network (Albers and Fuchs, 1987). These data suggested that integration of subunits occurs everywhere along a filament as opposed to strictly at one end or the other, consistent with recent findings of Ngai et al. (1990). In addition, a K14 mutant missing a COOH-terminal portion of the coiled-coil domain disrupted both newly formed and preexisting keratin filament networks, suggesting that the network is a dynamic one, with subunits capable of integrating into both new and existing filaments (Albers and Fuchs, 1987). When transient gene expression apparently subsided in the cells transfected with mutant keratin genes, seemingly new synthesis of endogenous keratin subunits led to formation of a de novo filament network surrounding the nucleus (Albers and Fuchs, 1987). Similar studies on amino-terminal coiled-coil mutants of K14 led to additional evidence suggestive of an association between the nuclear envelope and IFs (Albers and Fuchs, 1989). One possible explanation for these observations is that new keratin filament assembly may have a preference to occur at the nuclear envelope, and under conditions where this putative preference is manifested, subsequent growth of filaments would proceed toward the cytoplasmic membrane (Albers and Fuchs, 1989). This has also been suggested independently by Eckert et al. (1982), who conducted keratin filament assembly studies in the presence of nuclear mem-

EM data suggesting that the mass-per-unit length along the keratin filament can vary considerably by one to two protofibrils in width (Steven et al., 1983; Engel et al., 1985); and (*e*) our data demonstrating that under strongly denaturing conditions, a number of keratin subunit and filament intermediates coexist, suggesting that there may not be a linear sequence of events leading to filament formation. If under physiological conditions, new filament assembly preferentially takes place at the surface of the nucleus, then filaments could grow towards the cytoplasmic membrane by end-to-end addition of tetramer or octamer subunits (*curved arrows*). If lateral association of tetramers or octamers also takes place as indicated in the diagram (*straight arrows*), but at a somewhat lower frequency than end-to-end addition, some variation in mass-per-unit length would be generated along the growing keratin filament. Finally, assuming that end-to-end and lateral additions of subunits occur simultaneously under physiological conditions, growth of protofibrils (and/or protofilaments) could easily lead to addition of subunits throughout the length of the growing filament, as indicated in the diagram. Note that the model shown illustrates only addition and not removal, or exchange, of subunits. If the equilibrium between addition and removal of subunits does not greatly favor subunit addition, a dynamic flux of addition and removal could occur, leading to exchange of newly synthesized subunits with previously made ones (see Albers and Fuchs, 1987; Ngai et al., 1990). Hatched subunits indicate those subunits most recently added to the schematic growing filament.

branes, Georgatos and Blobel (1987), who observed IF fila-
ment assembly from a mixture of vimentin and nuclear (but
not cytoplasmic) membranes, and Vikstrom et al. (1989),
who used microinjection of vimentin protein to examine fila-
ment formation (for review, see Steinert and Liem, 1990).

Our in vitro assembly studies did not involve membrane
preparations and therefore our data only confirm a well-
established fact, namely that filament formation per se does
not appear to require the presence of any auxiliary proteins,
factors or organelles. Hence, our data do not address the is-
sue of whether there might be a preference for de novo fila-
ment assembly off the nuclear envelope under physiological
conditions. However, our new data on keratin subunit struc-
ture now enable us to provide a more detailed IF assembly
model, which allows for both de novo IF assembly at the nu-
clear envelope as well as subunit addition and exchange
throughout the length of a filament (Fig. 10 B). One way in
which apolar subunits could integrate throughout the length
of an IF, and still have IFs grow preferentially in a unilateral
direction would be if lateral subunit interactions could take
place under conditions where end-to-end interactions were
also permissible. In such a scenario, filaments could begin
to grow by end-to-end interactions emanating from an initia-
tion site, possibly the nuclear envelope. However, if lateral
interactions also took place simultaneously, then new
subunits could add throughout the length of the growing fila-
ment, a feature which is consistent with the gene transfection
data, as well as with recently published data on microinjec-
tion of IF proteins (Vikstrom et al., 1989). If lateral associa-
tions were slightly less favorable than end-to-end interac-
tions, a consequence of such an assembly process would be
the production of filaments with polymorphic mass-per-unit
length. Intriguingly, such polymorphism has been observed
in scanning transmission EM analysis of in vitro assembled
keratin IFs (Steven et al., 1983; Aebi et al., 1986). Finally,
while for simplicity, the model in Fig. 10 B only covers addi-
tion of new subunits, it is implicit that exchange of subunits
can, and almost certainly does, take place along the length
of the filament.

In summary, we have isolated and characterized the
subunits involved in the early stages of keratin filament for-
mation, and we have shown that these subunits are non-polar
in their structure. The equilibrium that we have uncovered
among monomers, heterodimers and heterotetramers under
strongly denaturing conditions is indicative that such equili-
briums might also exist for higher ordered structures under
more physiological conditions. This suggests that there may
not be a linear sequence of events leading to higher levels of
keratin filament assembly, but rather there may be a number
of associations occurring simultaneously. As future studies
are conducted, we hope to unravel these and other remaining
mysteries underlying the complex self-assembly of 20,000–
30,000 polypeptides into 10-nm fibers.

References

Aebi, U., W. E. Fowler, P. Rew, and T.-T. Sun. 1983. The fibrillar substruc-
ture of keratin filaments unraveled. J. Cell Biol. 97:1131–1143.

Aebi, U., J. Cohn, L. Buhle, and L. Gerace. 1986. The nuclear lamina is a
meshwork of intermediate-type filaments. Nature (Lond.). 323:560–564.

Aebi, U., M. Haner, J. Troncoso, R. Eichner, and A. Engel. 1988. Unifying
principles in intermediate filament (IF) structure and assembly. Pro-
toplasma. 145:73–81.

Ahmadi, B., and P. T. Speakman. 1978. Suberimidate crosslinking shows that
a rod-shaped low-cysteine high-helix protein prepared by limited proteolysis
of reduced wool has four protein chains. FEBS (Fed. Eur. Biochem. Soc.)
Lett. 94:365–367.

Albers, K., and E. Fuchs. 1987. The expression of mutant epidermal keratin
cDNAs transfected in simple epithelial and squamous cell carcinoma lines.
J. Cell Biol. 105:791–806.

Albers, K., and E. Fuchs. 1989. Expression of mutant keratin cDNAs in epithe-
lial cells reveals possible mechanisms for initiation and assembly of inter-
mediate filaments. J. Cell Biol. 108:1477–1493.

Chreighton, T. E. 1979. Electrophoretic analysis of the unfolding of proteins
by urea. J. Mol. Biol. 129:235–264.

Conway, J. F., and D. A. D. Parry. 1988. Intermediate filament structure. 3.
Analysis of sequence homologies. Int. J. Biol. Macromol. 10:79–98.

Coulombe, P. A., R. Kopan, and E. Fuchs. 1989. Expression of keratin K14
in the epidermis and hair follicle: insights into complex programs of differen-
tiation. J. Cell Biol. 109:2295–2312.

Crewther, W. G., L. M. Dowling, D. A. D. Parry, and P. M. Steinert. 1983.
The structure of intermediate filaments. Int. J. Biol. Macromol. 5:267–282.

Crick, F. H. C. 1953. The packing of alpha-helices: simple coiled-coils. Acta
Crystallogr. 6:689–697.

Eckert, B. S., R. A. Daley, and L. M. Parysek. 1982. Assembly of keratin onto
PtK1 cytoskeletons: evidence for an intermediate filament organizing center.
J. Cell Biol. 92:575–578.

Eichner, R., T.-T. Sun, and U. Aebi. 1986. The role of keratin subfamilies and
keratin pairs in the formation of human epidermal intermediate filaments. J.
Cell Biol. 102:1767–1777.

Engel, A., R. Eichner, and U. Aebi. 1985. Polymorphism of reconstituted hu-
man epidermal keratin filaments: determination of their mass-per-length and
width by scanning transmission electron microscopy (STEM). J. Ultrastruct.
Res. 90:323–335.

Fisher, D. Z., N. Chaudhary, and G. Blobel. 1986. CDNA sequencing of nu-
clear lamins A and C reveals primary and secondary structural homology to
intermediate filament proteins. Proc. Natl. Acad. Sci. USA. 83:6450–6454.

Franke, W. W., D. L. Schiller, and C. Grund. 1982. Protofilamentous and an-
nulare structures as intermediates during reconstitution of cytokeratin fila-
ments in vitro. Biol. Cell. 46:257–268.

Franke, W. W., D. L. Schiller, M. Hatzfeld, and S. Winter. 1983. Protein com-
plexes of intermediate-sized filaments: melting of cytokeratin complexes in
urea reveals different polypeptide separation characteristics. Proc. Natl.
Acad. Sci. USA. 80:7113–7117.

Fraser, R. D. B., T. P. McRae, D. A. D. Parry, and E. Suzuki. 1986. Inter-
mediate filaments in α-keratins. Proc. Natl. Acad. Sci. USA. 83:1179–1183.

Fraser, R. D. B., P. M. Steinert, and A. C. Steven. 1987. Meeting report: focus
on intermediate filaments. Trends Biochem. Sci. 12:43–45.

Fuchs, E., and D. Marchuk. 1983. Type I and type II keratins have evolved
from lower eukaryotes to form the epidermal intermediate filaments in mam-
malian skin. Proc. Natl. Acad. Sci. USA. 80:5857–5861.

Fuchs, E., S. Coppock, H. Green, and D. Cleveland. 1981. Two distinct classes
of keratin genes and their evolutionary significance. Cell. 27:75–84.

Fuchs, E., A. L. Tyner, G. J. Giudice, D. Marchuk, A. RayChaudhury, and
M. Rosenberg. 1987. The human keratin genes and their differential expres-
sion. Curr. Top. Dev. Biol. 22:5–34.

Geisler, N., and K. Weber. 1982. The amino acid sequence of chicken muscle
desmin provides a common structural model for intermediate filament pro-
teins. EMBO (Eur. Mol. Biol. Organ.) J. 1:1649–1656.

Geisler, N., E. Kaufmann, and K. Weber. 1985. Antiparallel orientation of the
two double-stranded coiled-coils in the tetrameric protofilament unit of inter-
mediate filaments. J. Mol. Biol. 182:173–177.

Geisler, N., M. Potschka, and K. Weber. 1986. Are the terminal domains in
intermediate filaments organized as octameric complexes? Reevaluation of
a recent suggestion. J. Ultrastruct. Mol. Struct. Res. 94:239–245.

Georgatos, S. D., and G. Blobel. 1987. Two distinct attachment sites for vimen-
tin along the plasma membrane and the nuclear envelope in avian erythro-
cytes: a basis for a vectorial assembly of intermediate filaments. J. Cell Biol.

105:105-115.

Giudice, G. J., and E. Fuchs. 1987. The transfection of human epidermal keratin genes into fibroblasts and simple epithelial cells: evidence for inducing a type I keratin by a type II gene. *Cell.* 48:453-463.

Gruen, L. C., and E. F. Woods. 1983. Structural studies on the microfibrillar proteins of wool. *Biochem J.* 209:587-595.

Hanukoglu, I., and E. Fuchs. 1982. The cDNA sequence of a human epidermal keratin: divergence of sequence but conservation of structure among intermediate filament proteins. *Cell.* 31:243-252.

Hanukoglu, I., and E. Fuchs. 1983. The cDNA sequence of a type II cytoskeletal keratin reveals constant and variable structural domains among keratins. *Cell.* 33:915-924.

Hatzfeld, M., and W. W. Franke. 1985. Pair formation and promiscuity of cytokeratins: formation in vitro of heterotypic complexes and intermediate-sized filaments by homologous and heterologous recombinations of purified polypeptides. *J. Cell Biol.* 101:1826-1841.

Hatzfeld, M., G. Maier, and W. W. Franke. 1987. Cytokeratin domains involved in heterotypic complex formation determined by in vitro binding assays. *J. Mol. Biol.* 197:237-255.

Hatzfeld, M., and K. Weber. 1990. The coiled coil of in vitro assembled keratin filaments is a heterodimer of type I and II keratins: use of site-specific mutagenesis and recombinant protein expression. *J. Cell Biol.* 110:1199-1210.

Henderson, D., N. Geisler, and K. Weber. 1982. A periodic ultrastructure in intermediate filaments. *J. Mol. Biol.* 155:173-176.

Ip, W., M. K. Hartzer, Y.-Y. S. Pang, and R. M. Robson. 1985. Assembly of vimentin in vitro and its implications concerning the structure of intermediate filaments. *J. Mol. Biol.* 183:365-375.

Jorcano, J. L., J. K. Franz, and W. W. Franke. 1984a. Amino acid sequence diversity between bovine epidermal cytokeratin polypeptides of the basic (type II) subfamily as determined from cDNA clones. *Differentiation.* 28:155-163.

Jorcano, J. L., M. Rieger, J. K. Franz, D. L. Schiller, R. Moll, and W. W. Franke. 1984b. Identification of two types of keratin polypeptides within the acidic cytokeratin subfamily I. *J. Mol. Biol.* 179:257-281.

Kaufman, E., K. Weber, and N. Geisler. 1985. Intermediate filament forming ability of desmin derivatives lacking either the amino-terminal 67 or the carboxy-terminal 27 residues. *J. Mol. Biol.* 185:733-742.

Landshulz, W. H., P. F. Johnson, and S. L. McKnight. 1988. The leucine zipper: a hypothetical structure common to a new class of DNA binding proteins. *Science (Wash. DC).* 240:1759-1764.

Lersch, R., and E. Fuchs. 1988. Sequence and expression of a type II keratin, K5, in human epidermal cells. *Mol. Cell. Biol.* 8:486-493.

Lersch, R., V. Stellmach, C. Stocks, G. Giudice, and E. Fuchs. 1989. Isolation, sequence, and expression of a human keratin K5 gene: transcriptional regulation of keratins and insights into pairwise control. *Mol. Cell. Biol.* 9:3685-3697.

Magin, T. M., M. Hatzfeld, and W. W. Franke. 1987. Analysis of cytokeratin domains by cloning and expression of intact and deleted polypeptides in *Escherichia coli. EMBO (Eur. Mol. Biol. Organ.) J.* 6:2607-2615.

Marchuk, D., S. McCrohon, and E. Fuchs. 1984. Remarkable conservation of structure among intermediate filament genes. *Cell.* 39:491-498.

Marchuk, D., S. McCrohon, and E. Fuchs. 1985. Complete sequence of a type I human keratin gene: presence of enhancer-like elements in the regulatory region of the gene. *Proc. Natl. Acad. Sci. USA.* 82:1609-1613.

McKeon, F. M., M. W. Kirschner, and D. Caputo. 1986. Homologies in both primary and secondary structure between nuclear envelope and intermediate filament proteins. *Nature (Lond.).* 319:463-468.

McLachlan, A. D. 1978. Coiled-coil formation and sequence regularities in the helical regions of α-keratins. *J. Mol. Biol.* 124:297-304.

McLachlan, A. D., and M. Stewart. 1975. Tropomyosin coiled-coil interactions: evidence for an unstaggered structure. *J. Mol. Biol.* 98:293-304.

McLachlan, A. D., and M. Stewart. 1982. Periodic charge distribution in the intermediate filament proteins desmin and vimentin. *J. Mol. Biol.* 162:693-698.

Milam, L., and H. P. Erickson. 1982. Visualization of a 21-nm axial periodicity in shadowed keratin filaments and neurofilaments. *J. Cell Biol.* 94:592-596.

Nagai, K., and H.-C. Thorgersen. 1987. Synthesis and sequence-specific proteolysis of hybrid proteins produced in *Escherichia coli. Methods Enzymol.* 153:461-481.

Nelson, W., and T.-T. Sun. 1983. The 50- and 58-kD keratin classes as molecular markers for stratified squamous epithelia: cell culture studies. *J. Cell Biol.* 97:244-251.

Ngai, J., T. R. Coleman, and E. Lazarides. 1990. Localization of newly synthesized vimentin subunits reveals a novel mechanism of intermediate filament assembly. *Cell.* 60:415-427.

Parry, D. A. D., W. G. Crewther, R. D. Fraser, and T. P. MacRae. 1977. Structure of α-keratin: structural implications of the amino acid sequence of the type I and type II chain segments. *J. Mol. Biol.* 113:449-454.

Parry, D. A. D., A. C. Steven, and P. M. Steinert. 1985. The coiled-coil molecules of intermediate filaments consist of two parallel chains in exact axial register. *Biochem. Biophys. Res. Commun.* 127:1012-1018.

Parry, D. A. D., A. E. Goldman, R. D. Goldman, and P. M. Steinert. 1987. Nuclear lamin proteins: common structures for paracrystalline, filamentous and lattice forms. *Int. J. Biol. Macromol.* 9:137-145.

Pauling, L., and R. B. Corey. 1953. Compound helical configurations of polypeptide chains: structure of proteins of the α-keratin type. *Nature (Lond.).* 171:59-61.

Potschka, M. 1986. Structure of intermediate filaments. *Biophys. J.* 49:129-130.

Quinlan, R. A., and W. W. Franke. 1982. Heteropolymer filaments of vimentin and desmin in vascular smooth muscle tissue and cultured baby hamster kidney cells demonstrated by chemical crosslinking. *Proc. Natl. Acad. Sci. USA.* 79:3452-3456.

Quinlan, R. A., and M. Stewart. 1987. Crystalline tubes of myosin subfragment-2 showing the coiled-coil and molecular interaction geometry. *J. Cell Biol.* 105:403-415.

Quinlan, R. A., J. A. Cohlberg, D. L. Schiller, M. Hatzfeld, and W. W. Franke. 1984. Heterotypic tetramer (A_2D_2) complexes of non-epidermal keratins isolated from cytoskeletons of rat hepatocytes and hepatoma cells. *J. Mol. Biol.* 178:365-388.

Quinlan, R. A., M. Hatzfeld, W. W. Franke, A. Lustig, T. Schulthess, and J. Engel. 1986. Characterization of dimer subunits of intermediate filament proteins. *J. Mol. Biol.* 192:337-349.

Rosenberg, A. H., B. N. Lade, D.-S. Chui, S.-W. Lin, J. J. Dunn, and F. W. Studier. 1987. Vectors for selective expression of cloned DNAs by T7 RNA polymerase. *Gene.* 56:125-135.

Steinert, P. M., and R. K. H. Liem. 1990. Intermediate filament dynamics. *Cell.* 60:521-523.

Steinert, P. M., W. W. Idler, and S. B. Zimmermann. 1976. Self assembly of bovine epidermal keratin filaments in vitro. *J. Mol. Biol.* 108:547-567.

Steinert, P. M., R. H. Rice, D. R. Roop, B. L. Trus, and A. C. Steven. 1983. Complete amino acid sequence of a mouse epidermal keratin subunit and implications for the structure of intermediate filaments. *Nature (Lond.).* 302: 794-800.

Steinert, P. M., D. A. D. Parry, E. Racoosin, W. Idler, A. Steven, B. Trus, and D. Roop. 1984. The complete cDNA and deduced amino acid sequence of a type II mouse epidermal keratin of 60,000 Da: analysis of sequence differences between type I and type II keratins. *Proc. Natl. Acad. Sci. USA.* 81:5709-5713.

Steinert, P. M., A. C. Steven, and D. R. Roop. 1985. The molecular biology of intermediate filaments. *Cell.* 42:411-419.

Stellmach, V. M., and E. Fuchs. 1989. Exploring the mechanisms underlying cell type-specific and retinoid-mediated expression of keratins. *New Biologist.* 1:305-317.

Steven, A., J. Hainfeld, B. Trus, J. Wall, and P. Steinert. 1983. Epidermal keratin filaments assembled in vitro have masses-per-unit length that scale according to average subunit masses: structural basis for homologous packing of subunits in intermediate filaments. *J. Cell Biol.* 97:1939-1944.

Stewart, M., R. A. Quinlan, and R. D. Moir. 1989. Molecular interactions in paracrystals in a fragment corresponding to the α-helical coiled-coil rod portion of glial fibrillary acidic protein: evidence for an antiparallel packing of molecules and polymorphism related to intermediate filament structure. *J. Cell Biol.* 109:225-234.

Stoler, A., R. Kopan, M. Duvic, and E. Fuchs. 1988. The use of monospecific antibodies and cRNA probes reveals abnormal pathways of terminal differentiation in human epidermal diseases. *J. Cell Biol.* 107:427-446.

Studier, F. W., and B. A. Moffatt. 1986. Use of bacteriophage T7 RNA polymerase to direct selective high-level expression of cloned genes. *J. Mol. Biol.* 189:113-130.

Sun, T.-T., and H. Green. 1978. Keratin filaments in cultured human epidermal cells. *J. Biol. Chem.* 253:2053-2060.

Sun, T.-T., R. Eichner, A. Schermer, D. Cooper, W. G. Nelson, and R. A. Weiss. 1984. The transformed phenotype. *In* The Cancer Cell. Vol. 1. A. Levine, W. Topp, G. van de Woude, and J. D. Watson, editors. Cold Spring Harbor Laboratory, Cold Spring Harbor, New York. 169-176.

Towbin, H., T. Staehelin, and J. Gordon. 1979. Electrophoretic transfer of proteins from polyacrylamide gels onto nitrocellulose sheets: procedure and some applications. *Proc. Natl. Acad. Sci. USA.* 81:4683-4687.

Tsao, T. C. 1953. Fragmentation of the myosin molecule. *Biochimica Biophys. Acta.* 11:366-382.

Vikstrom, K. L., G. G. Borisy, and R. D. Goldman. 1989. Dynamic aspects of intermediate filament networks in BHK-21 cells. *Proc. Natl. Acad. Sci. USA.* 86:549-553.

Weber, K., and N. Geisler. 1987. Biochemistry and molecular structure of intermediate filaments. *In* Nature and Function of Cytoskeletal Proteins in Motility and Transport. Gustave Fischer, editor. Springer-Verlag, Stuttgart, W. Germany. 251-260.

Wong, K. P., and C. Tanford. 1973. Denaturation of carbonic anhydrase B by guanidine hydrochloride. *J. Biol. Chem.* 248:8518-8523.

Woods, E. F., and A. S. Inglis. 1984. Organization of the coiled-coils in the wool microfibril. *Int. J. Biol. Macromol.* 6:277-283.